RESEARCH TRIANGLE INSTITUTE

RTI/2467

NASA CR-172338

EFFECTS OF AIRCRAFT AND FLIGHT PARAMETERS ON ENERGY-EFFICIENT PROFILE DESCENTS IN TIME-BASED METERED TRAFFIC

Prepared under Contract No. NAS1-17023

By

Fred R. DeJarnette

Center for Systems Engineering
Research Triangle Institute
Research Triangle Park, North Carolina 27709

for

NASA

National Aeronautics and Space Administration
Langley Research Center
Hampton, Virginia 23665

February 1984

RTI/2467

NASA CR-172338

EFFECTS OF AIRCRAFT AND FLIGHT PARAMETERS ON ENERGY-EFFICIENT PROFILE DESCENTS IN TIME-BASED METERED TRAFFIC

Prepared under Contract No. NAS1-17023

By

Fred R. DeJarnette

Center for Systems Engineering
Research Triangle Institute
Research Triangle Park, North Carolina 27709

for

National Aeronautics and Space Administration
Langley Research Center
Hampton, Virginia 23665

February 1984

ACKNOWLEDGEMENTS

This report was prepared by the Center for Systems Engineering, Research Triangle Institute, Research Triangle Park, North Carolina, under contract NAS1-17023. The research is under the direction of personnel in the Flight Control Systems Division, Langley Research Center, National Aeronautics and Space Administration. Mr. Leonard Credeur is the Langley Technical Representative for the contract.

Significant contributions to the research in this report have been made by Mr. Leonard Credeur of Langley Research Center and Mr. William R. Capron of Kentron International, Inc. Dr. Fred DeJarnette, consultant to Research Triangle Institute and professor of Mechanical and Aerospace Engineering at North Carolina State University, is the author of the report, and he gratefully acknowledges the contributions of the following Research Triangle Institute personnel:

Dr. Dershuen Tang for his assistance with the computer algorithm and many helpful discussions;

Ms. Mary (Liz) Gordon for programming the algorithm and obtaining the results used in this report;

Ms. Christina M. Davis, presently with IBM, for her assistance in formulating the profile descents; and

Ms. Sharon McLamb for typing the manuscript.

TABLE OF CONTENTS

SUMMARY

The National Aeronautics and Space Administration and the Federal Aviation Administration have developed concepts which save fuel while preserving airport capacity by combining time-based metering with profile descent procedures. NASA conducted experiments where an aircraft descended from cruise altitude in a fuel-efficient manner by flying with idle thrust and a clean (low drag) configuration. This report describes a computer algorithm developed to provide the flight crew with the information needed to fly from an entry fix (about 100 n.mi. from the airport) to a metering fix (about 25 n.mi. from the airport) and arrive there at a predetermined time, altitude, and airspeed. Additional information is calculated for the flight from the metering fix to an aim point near the airport. The algorithm was developed for use in an air traffic simulation to model the dynamics of aircraft performing flight-idle profile descents.

The flight path is divided into several descent and deceleration segments. Descents are performed at constant Mach numbers or calibrated airspeed, whereas decelerations occur at constant altitude. The time and distance associated with each segment are calculated from point-mass equations of motion for a clean configuration with idle thrust (except for one constant speed segment where non-idle thrust must be used). An iterative process is used to determine the metering-fix altitude, within a prescribed altitude window, and another iterative process determines the Mach number/calibrated airspeed combination for the descent which allows the aircraft to arrive at the metering fix at a prescribed time, altitude, and speed. The calculation for time and distance can be simplified by using approximate relations for variation of the rate of descent and deceleration.

Results for the B-737 aircraft show that wind and non-standard atmospheric properties have a large effect on the flight path and cannot be neglected. Uncertainty in the descent Mach number was found to have a large effect on the predicted flight time, whereas uncertainty in the weight was insignificant. A range of combinations of Mach number and calibrated

airspeed is possible for the descent segments leading to the metering fix. However, only small changes in the fuel consumed were observed for this range of combinations. Therefore, a combination based on flexibility for scheduling seems preferable. Profile descents for heavier aircraft (in the range of the B-747) were found to be similar to those for the B-737.

1.0 INTRODUCTION

The increasing cost of fuel and air traffic control problems motivated the Federal Aviation Administration to develop a concept called local flow management/profile descent. This concept saves fuel and preserves airport capacity by combining time-based metering with profile descent procedures. Presently the flight crew is responsible for the altitude and speed objective while ATC is responsible for time delivery at the metering fix. However, both the pilot and controller have little or no guidance to assist them. A computer algorithm is developed in this report to provide the information needed to fly from an entry fix through a profile descent to a metering fix and arrive there at a predetermined time, altitude, and airspeed. In addition, an algorithm is included to determine the altitude of the metering fix such that the aircraft will arrive at an aim point within the terminal area with a prescribed altitude, airspeed, and distance from the metering fix. The algorithm was developed for use in an air traffic simulation to model the dynamics of aircraft performing flight-idle profile descents.

The computational algorithm divides the flight path from the entry fix to the metering fix into the five segments illustrated in Fig. 1-1. Four additional segments are used to simulate the flight path from the metering fix to the aim point. The segments are numbered in the order of their calculation which are reversed from the order they occur. Segment 5 starts at entry fix with cruise altitude (h_c) and Mach number (M_c) and decelerates at constant altitude with idle thrust until the prescribed descent Mach number (M_d) is reached. Segment 4 is a constant speed and altitude path to the beginning of descent. In Segment 3 the aircraft descends with idle thrust

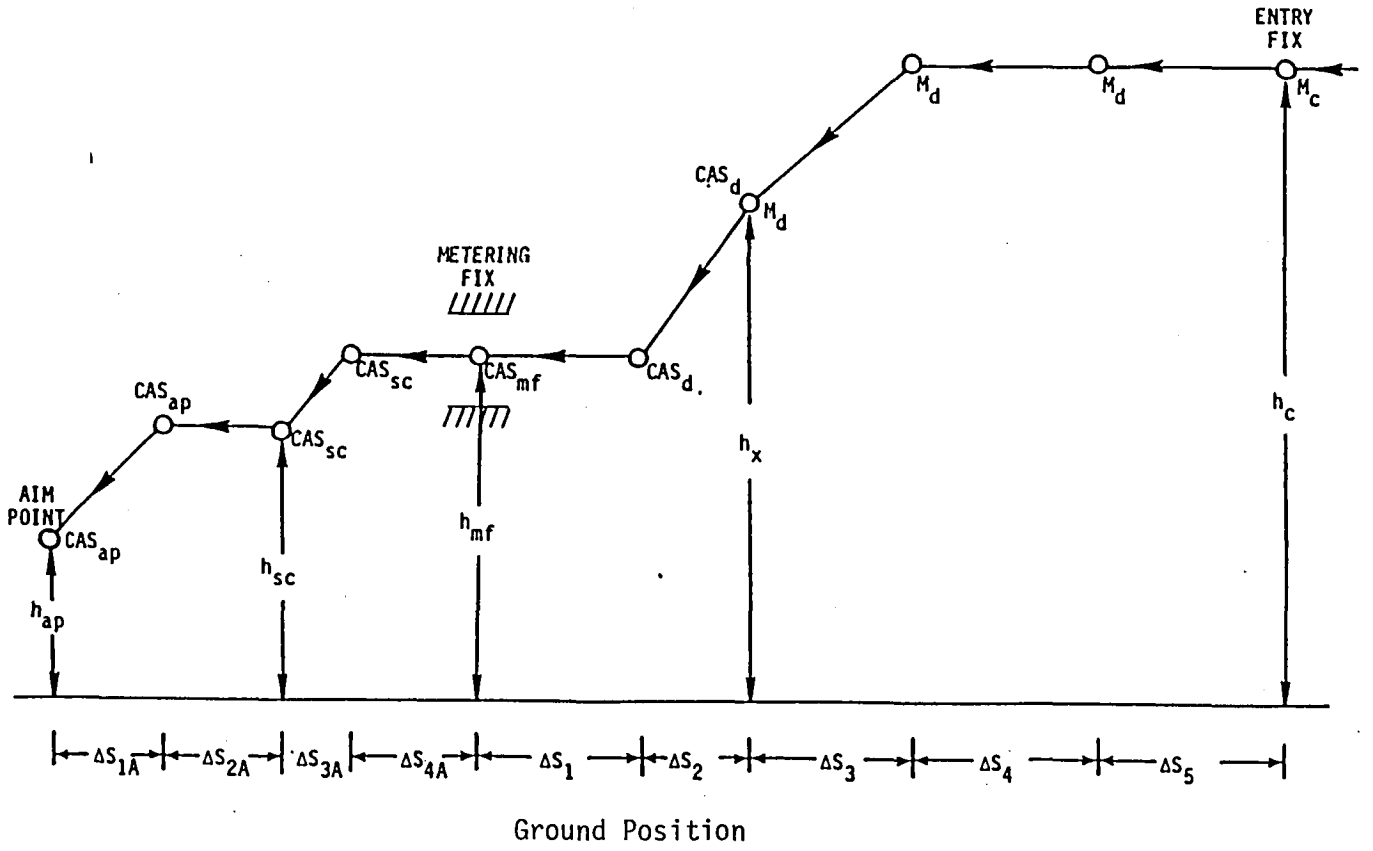

Figure 1-1. Geometry of flight-path segments.

and a clean configuration (low drag) at an attitude which maintains constant M_d. As the altitude decreases, the calibrated airspeed increases. When the calibrated airspeed reaches a prescribed value (CAS_d), Segment 3 stops and Segment 2 begins. Still maintaining idle thrust and a clean configuration, the aircraft descends at constant CAS_d until the metering-fix altitude is reached. Segment 1 is a deceleration at constant altitude (h_{mf}) from CAS_d to the designated metering-fix calibrated airspeed (CAS_{mf}). If an ideal flight path were flown, the aircraft would arrive at the metering fix at the prescribed time.

The region from the metering fix to the aim point begins with Segment 4A where the aircraft continues to decelerate until the prescribed speed control airspeed (CAS_{sc}) is reached. Segment 3A is a descent at CAS_{sc} from h_{mf} to the speed control altitude (h_{sc}). Segment 2A decelerates the aircraft from CAS_{sc} to the calibrated airspeed designated for the aim point (CAS_{ap}). Then segment 1A is a descent from h_{sc} to the aim point altitude (h_{ap}) at constant CAS_{ap}. If an ideal flight path were flown, the aircraft would arrive at the aim point altitude at a prescribed distance from the metering fix.

For all the segments described above, decelerations occur at constant altitude and descents have constant calibrated airspeed or Mach number. Clean configurations and flight-idle thrust are used throughout the flight path except for Segment 4 where the aircraft must use non-idle thrust to maintain constant Mach number (M_d). Time-metering aircraft to fly profile descents reduces low altitude vectoring and fuel consumption, and helps alleviate airport noise since the aircraft fly longer at higher altitudes near the airport.

The Boeing Commercial Airplane Company developed an elaborate computer program (Ref. 1) to calculate profile descents. However, it requires a sophisticated computer to perform the calculations. Much simpler techniques were developed by Knox and Cannon (Ref. 2) and Knox (Ref. 3) which can be used on small programmable calculators. On the other hand, some of the approximations, particularly the rate of descent approximations, used in their analyses can lead to significant errors in some cases.

This report describes a computer program to calculate the profile descents described above. It is simpler than that of Ref. 1, but more accurate than the techniques used in Refs. 2 and 3. Results are presented for the B-737 and typical heavy-class aircraft; and the effects of winds, nonstandard atmospheres, and optimal paths for minimum fuel consumption are discussed.

2.0 SYMBOLS

a	local speed of sound, ft/sec
a_o	standard sea-level speed of sound, kts
$A_0, A_1, \ldots, A_4$	coefficients for drag coefficient, Eq. 4
CAS	calibrated airspeed, kts
C_D	drag coefficient
C_L	lift coefficient
D	drag force, lb and distance, n.mi.
F	engine thrust, lb
g	gravitational acceleration, 32.174 ft/sec^2
h	altitude, ft
L	lift force, lb
M	Mach number
p	atmospheric pressure, lb/ft^2
p_0^1	non-standard sea-level pressure, lb/ft^2
R	gas constant for air, 1716 ft^2/sec^2/ °R
S	wing area, ft^2
t	time, sec
T	atmospheric temperature, °R
V	true airspeed, ft/sec
V_g	ground speed, ft/sec
V_W	wind speed, ft/sec
w_f	fuel weight, lb
W	aircraft weight, lb
X, Y	Cartesian coordinates on ground with X pointing North and Y pointing East, ft
$\dot{X}, \dot{Y}$	components of ground speed in X and Y directions, respectively, ft/sec
α	temperature lapse rate, °R/ft
γ	inclination of flight path relative to the local horizontal, degrees
$\bar{\gamma}$	ratio of specific heats (1.4 for air)
ΔS	distance interval, n.mi.

Δt	time interval, sec
ρ	atmospheric density, slug/ft^3
θ	track heading measured clockwise from X-axis, degrees
ψ	aircraft heading measured clockwise from X-axis, degrees
ψ_W	wind angle measured clockwise from X-axis, degrees

Subscripts

ap	aim point
avg	average value
c	cruise conditions
d	descent conditions
f	final value
g	along the ground
i	subscript for segment
max	maximum value
mf	conditions at metering fix
min	minimum value
req	value required
sc	speed control segment
t	value at stagnation point
TOT	total value
W	wind value
x	conditions at the cross-over altitude
0	sea-level or initial value
1	conditions at 36,089 ft

3.0 ANALYSIS

The methods used here to calculate the deceleration and descent segments are quite different from those used by Knox and Cannon (Ref. 2). For these segments, the equations of motion along and normal to the flight path are needed. Consider the sketch below.

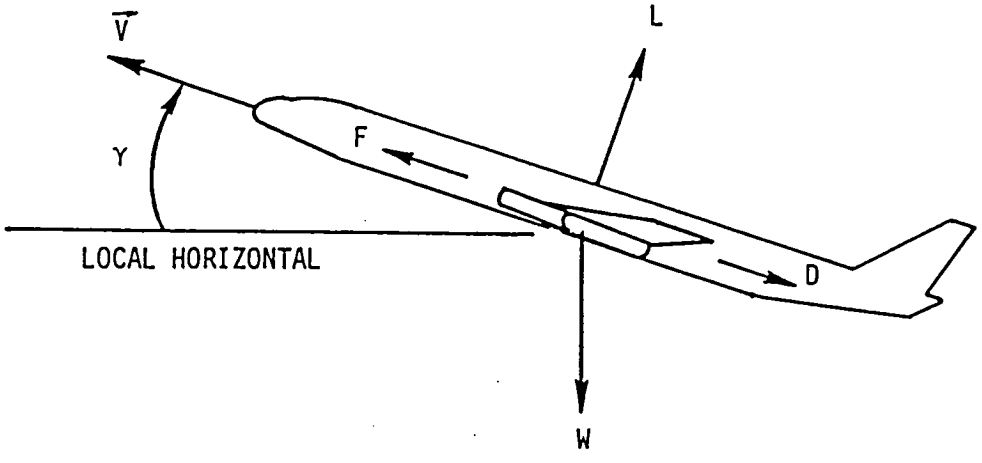

Figure 3-1. Forces on an aircraft.

Newton's second law along the flight path gives (Ref. 4):

$$\frac{W}{g}\frac{dV}{dt} = F - D - W \sin \gamma \qquad (1)$$

For level flight, $\gamma = 0$ and Eq. 1 gives:

$$\frac{W}{g}\frac{dV}{dt} = F - D$$

or

$$\frac{dV}{dt} = (F - D)\frac{g}{W} \quad . \tag{2}$$

This equation gives the acceleration (negative of the deceleration) at constant altitude. The idle thrust (F) and drag (D) are needed to calculate the deceleration and they are obtained by the methods used in Ref. 1. The thrust is calculated from a two-dimensional interpolation of tabulated data of idle thrust as a function of altitude and Mach number. The drag is given by

$$D = C_D \frac{1}{2} \rho V^2 S \tag{3}$$

where ρ is the air density and S is the wing area. The drag coefficient, C_D, is obtained from fourth-degree polynomial curve fits to tabulated data of C_D as a function of Mach number and lift coefficient C_L.

$$C_D = A_0 + A_1 C_L + A_2 C_L^2 + A_3 C_L^3 + A_4 C_L^4 \tag{4}$$

The coefficients A_0, A_1, A_2, A_3, and A_4 are determined by interpolating between values tabulated as a function of Mach numbers.

For descent segments, the rate of climb is

$$\frac{dh}{dt} = V \sin \gamma \quad . \tag{5}$$

Also, the acceleration can be written as

$$\frac{dV}{dt} = \frac{dV}{dh}\frac{dh}{dt} \quad . \tag{6}$$

Substitute for sin from Eq. 5 and $\frac{dV}{dt}$ from Eq. 6 into Eq. 1 to obtain

$$\frac{W}{g}\frac{dV}{dh}\frac{dh}{dt} = F - D - \frac{W}{V}\frac{dh}{dt}$$

which can be rearranged to give

$$\frac{dh}{dt} = \frac{(F - D)}{W\left(\frac{1}{g}\frac{dV}{dh} + \frac{1}{V}\right)} . \tag{7}$$

This equation is used to determine the rate of climb for descent segments. Expressions for $\frac{dV}{dh}$ for constant Mach and calibrated airspeed segments are given in Appendix C. The equation of motion normal to the flight path is (Ref. 4):

$$\frac{W}{g} V \frac{d\gamma}{dt} = L - W \cos \gamma . \tag{8}$$

For small values of $|\gamma|$ and $\left|\frac{d\gamma}{dt}\right|$, this equation can be approximated by

$$L = W. \tag{9}$$

Since lift (L) is related to the lift coefficient (C_L) by

$$L = C_L \frac{1}{2} \rho V^2 S, \tag{10}$$

Eq. 9 gives the lift coefficient as

$$C_L = \frac{2W}{\rho V^2 S} . \tag{11}$$

This equation is used to calculate C_L which, in turn, is used in the calculation of the drag coefficient.

The atmospheric density ρ can be obtained from the pressure and temperature by the ideal-gas equation of state

$$\rho = \frac{p}{RT} \tag{12}$$

where R is the gas constant for air and p and T are functions of altitude (see Appendix A).

3.1 Methods Used to Calculate Time and Distance

Consider the segments of the profile descent without wind effects for now. Wind effects will be considered later. Here the total ground distance traveled is ΔS_{TOT} and the track heading is θ. With no wind the airplane heading ψ is the same as the track heading.

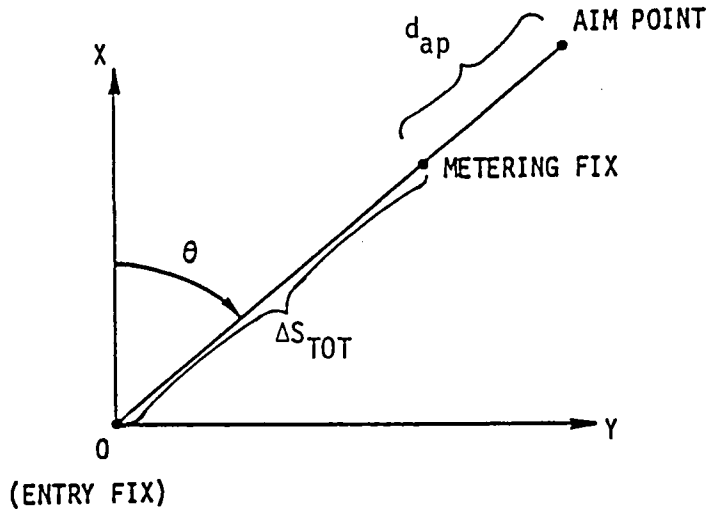

Figure 3-2. Ground path for no wind.

Now $\Delta S_{TOT} = \sum_{i=1}^{5} \Delta S_i$ and $\Delta t_{TOT} = \sum_{i=1}^{5} \Delta t_i$ for the total distance (ΔS_{TOT}) and total time (Δt_{TOT}) required to fly from the entry fix to the metering fix. Four additional segments must be added to fly from the metering fix to the aim point.

Consider ΔS_i and Δt_i for each segment for a prescribed value of ΔS_{TOT}.

3.1.1 Deceleration Segments at Constant Altitude. - The aircraft decelerates with idle thrust in a clean configuration from a prescribed CAS or M to a smaller value at the end of the segment.

From Eq. B-7 in Appendix B, the corresponding true airspeeds can be determined from CAS or M. Then the time required for this segment is calculated by numerically integrating Eq. 2, i.e.

$$\Delta t_i = \int \frac{dV}{(dV/dt)} = \int_{V_0}^{V_f} \frac{W \; dV}{(F - D)g} \tag{13}$$

and the distance traveled is calculated from

$$\Delta S_i = \int \frac{V \; dV}{(dV/dt)} = \int_{V_0}^{V_f} \frac{W \; V \; dV}{(F - D)g} \tag{14}$$

where V_0 is true airspeed at the beginning and V_f is the true airspeed at the end of the segment. The integrals above are evaluated numerically using Simpson's rule.

3.1.2 Descent at Constant Calibrated Airspeed. - The rate of climb is given by Eq. 7 as

$$\frac{dh}{dt} = \frac{F - D}{W\left(\frac{1}{g}\frac{dV}{dh} + \frac{1}{V}\right)} .$$

The right side of this equation depends on CAS and h only since $\frac{dV}{dh}$ is given by Eq. C-1 in Appendix C. Therefore, the time Δt_i is calculated numerically by using Eq. 7 in the following integral:

$$\Delta t_i = \int_{h_0}^{h_f} \frac{dh}{(dh/dt)} = \int_{h_0}^{h_f} \frac{W\left(\frac{1}{g}\frac{dV}{dh} + \frac{1}{V}\right) dh}{(F - D)} \tag{15}$$

where h_0 is the altitude at the beginning and h_f is the altitude at the end of the segment.

The distance ΔS_i is calculated numerically also by using Eq. 7 in the following integral:

$$\Delta S_i = \int V\,dt = \int_{h_0}^{h_f} \frac{V\,dh}{(dh/dt)} = \int_{h_0}^{h_f} \frac{W\left(\frac{1}{g}\frac{dV}{dh} + \frac{1}{V}\right) V\,dh}{(F - D)} \quad . \tag{16}$$

3.1.3 Descent at Constant Mach Number. - The technique here is the same as that above except that $\frac{dV}{dh}$ is dependent on M_d and h, and is given by Eq. C-2 in Appendix C. Therefore,

$$\Delta t_3 = \int_{h_c}^{h_x} \frac{dh}{(dh/dt)} = \int_{h_c}^{h_x} \frac{W\left(\frac{1}{g}\frac{dV}{dh} + \frac{1}{V}\right) dh}{(F - D)} \tag{17}$$

where h_c is the cruise altitude at the entry fix and h_x is the cross-over altitude which depends on M_d and CAS_d only (see Appendix B). For this segment V is dependent on M_d and h only. The distance here is similarly

$$\Delta S_3 = \int_{h_c}^{h_x} \frac{V\,dh}{(dh/dt)} = \int_{h_c}^{h_x} \frac{W\left(\frac{1}{g}\frac{dV}{dh} + \frac{1}{V}\right) V\,dh}{(F - D)} \quad . \tag{18}$$

The four integrals above for the descent segments are calculated numerically using the trapezoidal rule with increments in altitude as the independent variable.

3.1.4 Constant Speed and Altitude. - This segment is actually calculated after segment 5 because ΔS_5 is needed here. Since ΔS_{TOT} is prescribed, then

$$\Delta S_4 = \Delta S_{TOT} - (\Delta S_1 + \Delta S_2 + \Delta S_3 + \Delta S_5) \tag{19}$$

and

$$\Delta t_4 = \frac{\Delta S_4}{V_4} \tag{20}$$

where V_4 is the velocity corresponding to M_d at entry fix altitude (h_c).

The total time for the profile descent from entry fix to metering fix is $\Delta t_{TOT} = \sum_{i=1}^{5} \Delta t_i$. For prescribed values of ΔS_{TOT}, h_c, M_d, CAS_d, h_{mf}, and CAS_{mf}, the relations above can be used to calculate Δt_{TOT}. However, the proper combination of M_d and CAS_d must be determined which will make $\Delta t_{TOT} = \Delta t_{req}$.

The specific aircraft parameters which must be known to point-mass calculate the aircraft's flight-idle profile-descent path are:

1. Aircraft weight, W
2. Wing-reference area, S
3. Maximum and minimum Mach number and calibrated airspeed for aircraft in descent
4. Idle thrust as a function of altitude and Mach number
5. Coefficients for drag coefficient, Eq. 4, as a function of Mach number
6. Fuel flow rate as a function of altitude, Mach number, and thrust is needed if fuel consumption is desired. Note that Segment 4 required non-idle thrust whereas the other segments use idle thrust.

3.2 Method Used to Calculated M_d/CAS_d Combinations for Descent

An iterative method is used to determine the combination of M_d and CAS_d for Segments 2 and 3 which will make $\Delta t_{TOT} = \Delta t_{req}$ for the region between the entry fix and the metering fix. For a given aircraft, minimum and maximum values of M and CAS are prescribed. The technique used is:

(1) Starting with $M_d = M_{min}$, use CAS_{max} to calculate Δt_{min} and CAS_{min} to calculate Δt_{max} for this value of M_d. If $\Delta t_{req} < \Delta t_{min}$ or $\Delta t_{req} > \Delta t_{max}$, a profile descent cannot be performed at this M_d and the computer program jumps to step (4) below. If $\Delta t_{req} > \Delta t_{max}$, some other means of delay would be required.

(2) For the M_d in step (1), calculate the corresponding value of CAS_d which makes $|\Delta t_{TOT} - \Delta t_{req}| < 3$ sec. This is done iteratively using the modified regula falsi method (Ref. 5). Convergence is usually obtained in 3 iterations or less. It was found that this method always converged, whereas Newton's method diverged for some cases. The convergence criterion of 3 sec was chosen as a compromise between the number of iterations required and the accuracy of the calculated results.

(3) If $\frac{\Delta t_{req} - \Delta t_{min}}{\Delta t_{max} - \Delta t_{min}} > 0.3$, the current values of M_d and CAS_d are the combination selected. The lower limit of 0.3 means the difference between the desired metering-fix arrival time and the minimum arrival time is 30% of the span of time control for the current value of M_d. The 30% proportionality constant was chosen based on the assumption that delay, rather than advancement, is prevalent. This constant could be changed to any other value which may be determined to be more appropriate for local conditions.

(4) If $M_d \geq M_{max}$, stop. Otherwise, increase M_d by 0.01 and return to step (1). The criterion used in step (3) was chosen so that the profile descent would be performed at the smallest value of M_d which gave Δt_{req} to lie more than 0.3 between the maximum and minimum values for this M_d. This allows for more delay than a speed up. The minimum value of M_d generally produces minimum fuel consumption because the thrust required, and hence fuel consumption, in Segment 4 is minimized.

3.3 Effects of Wind

It is assumed that both wind speed and direction vary linearly with altitude and two gradient regions may be specified. The wind affects the ground speed and aircraft heading as well as the time required to arrive at the metering fix. For the computations here, the track heading (θ) is assumed constant throughout the profile descent. Therefore, the aircraft heading (ψ) will change during the profile descent. Consider the velocity vector diagram below

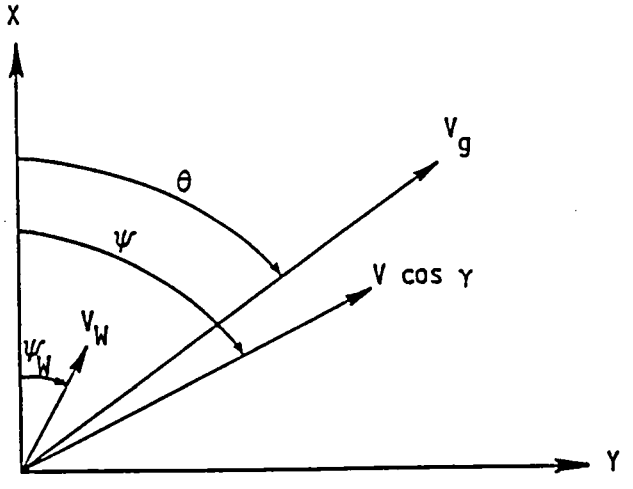

Figure 3-3. Velocity diagram on ground.

where

V = true airspeed

$V \cos\gamma$ = component of true airspeed parallel to the ground

ψ = aircraft heading

V_g = ground speed

θ = track heading (constant)

V_W = wind speed

ψ_W = wind angle = wind direction + 180°.

From the diagram, V_g is the sum of the components of V cos γ and V_W along the direction of V_g,

$$V_g = V \cos\gamma \cos(\psi-\theta) + V_W \cos(\theta-\psi_W) \tag{21}$$

where $(\psi-\theta)$ is the "crab" angle of the aircraft. It is assumed to be sufficiently small that

$$\cos(\psi-\theta) \approx 1.$$

In addition, $|\gamma|$ is sufficiently small that $\cos\gamma \approx 1$.

Then

$$V_g \approx V + V_W \cos(\theta-\psi_W) \tag{22}$$

and the ground distance traveled is

$$\Delta S = \int V_g dt = \int V\,dt + \int V_W \cos(\theta-\psi_W)\,dt$$

$$= (\Delta S)_{\substack{NO \\ WIND}} + \int V_W \cos(\theta-\psi_W)\,dt. \tag{23}$$

This relation can be used to correct the $(\Delta S)_{\substack{NO \\ WIND}}$ for the wind effects. (Note that $V_W \cos(\theta - \psi_W)$ is the tail wind in the diagram.) The time Δt_i is evaluated in the same fashion as no wind except for Segment 4.

Segment 1

Since the altitude is constant, V_W and ψ_W are constant and evaluated at h_{mf}. Thus

$$\Delta S_1 = (\Delta S_1)_{\substack{NO \\ WIND}} + V_W \cos(\theta-\psi_W)\,\Delta t_1. \tag{24}$$

Segment 2

Assume the wind speed and direction to be the same as that at the average altitude for this segment, i.e., $h_{avg} = \frac{h_{mf} + h_x}{2}$. Then (25)

$$\Delta S_2 = (\Delta S_2)_{\substack{NO \\ WIND}} + V_W \cos(\theta - \psi_W)\, \Delta t_2$$

Segment 3

Here also evaluate V_W and ψ_W at $h_{AVG} = \frac{h_x + h_c}{2}$, then

$$\Delta S_3 = (\Delta S_3)_{\substack{NO \\ WIND}} + V_W \cos(\theta - \psi_W)\, \Delta t_3 \qquad (26)$$

Segment 4 (Constant Altitude, h_c)

$\Delta S_4 = \Delta S_{TOT} - (\Delta S_1 + \Delta S_2 + \Delta S_3 + \Delta S_5)$; but also

$\Delta S_4 = V_4 \Delta t_4 + V_W \cos(\theta - \psi_W)\, \Delta t_4$.

Therefore

$$\Delta t_4 = \frac{\Delta S_4}{V_4 + V_W \cos(\theta - \psi_W)} . \qquad (27)$$

Segment 5 (Constant Altitude, h_c; this segment is calculated before Segment 4)

$$\Delta S_5 = (\Delta S_5)_{\substack{NO \\ WIND}} + V_W \cos(\theta - \psi_W)\, \Delta t_5 . \qquad (28)$$

Segments 1A, 2A, 3A, and 4A are similar to Segments 1 or 2.

3.4 Method to Calculate Metering-Fix Altitude and Segments from Metering Fix to Aim Point

The parameters input to the computer program relative to these calculations are:

(1) D_{ap}, distance from metering fix to the aim point

(2) D_{sc}, distance from metering fix to the beginning of a speed control segment, Segment 2A. $D_{sc} = \Delta S_{3A} + \Delta S_{4A}$

(3) CAS at metering fix, aim point, and for Segment 3A

(4) Altitude window at metering fix

(5) h_{ap}, altitude at aim point.

The four segments from the metering fix to the aim point are shown in Fig. 1-1. Segment 4A is a deceleration from CAS_{mf} at the metering fix altitude to CAS_{sc}, then the aircraft descends until the distance from the metering fix reaches D_{sc} (Segment 3A). At this point a constant altitude deceleration is performed until CAS_{ap} is reached (Segment 2A), and then a descent to h_{ap}. However, the metering-fix altitude (h_{mf}) required to reach the aim point at the prescribed distance D_{ap} is unknown.

Initially, maximum and minimum values of D_{ap} are calculated using the prescribed altitude window at the metering fix (maximum and minimum values of h_{mf}). If the prescribed value of D_{ap} lies between these bounds, the modified regula falsi method (Ref. 5) is used to calculate h_{mf}. If the input value of D_{ap} is outside these bounds, D_{ap} is changed to the nearest extremum value so that the profile descent computations for the segments between the entry fix and metering fix can be performed.

3.5 Influence of Parameters on Δt_{TOT}

The separate effects of the following parameters on Δt_{TOT} are calculated by changing each parameter by a small percentage and calculating the change in Δt_{TOT}:

h_{mf}, M_d, CAS_d, h_c, M_c, ΔS_{TOT}, W, ψ_w, and V_w.

When linear these effects can be considered as partial derivatives of Δt_{TOT} with respect to each of the parameters above while holding the remaining parameters constant. A description of the computer program is given in Appendix D.

3.6 Tracking Profile Descents

After the profile descent has been determined, and the pertinent parameters printed, a tracking subprogram is called which calculates the aircraft's position, heading, airspeed, ground speed, rate of climb, and flight path angle from the horizontal for prescribed integration time intervals. The wind effects are included in this subprogram also. The tracking starts at the entry fix and tracks the aircraft until it arrives at the aim point. The accuracy of the tracking computations is dependent on the prescribed integration step size in time, Δt.

The methods used to calculate the tracking parameters in each segment are the same as those described earlier to determine the profile descent. Additional considerations are needed, however, to calculate the aircraft heading with wind effects in the tracking subprogram. Since the wind changes the aircraft heading from the track heading, a new aircraft heading is calculated in each integration step. The change in heading is calculated by the method described in Ref. 6 for a coordinated turn. This method involves banking the aircraft to an appropriate angle for the turn within the constraints of the bank angle and time rate of change of bank angle for that aircraft. This part of the tracking subprogram was developed in Ref. 6.

To understand the algorithm used for the computations, the equations used to calculate the ground speed and track heading from the airspeed and aircraft heading are given below. (Refer to Fig. 3-3.)

$$\dot{X} = V \cos\gamma \cos\psi + V_W \cos\psi_W \tag{29}$$

$$X = \int \dot{X}\, dt \tag{30}$$

$$\dot{Y} = V \cos\gamma \sin\psi + V_W \sin\psi_W \tag{31}$$

$$Y = \int \dot{Y}\, dt \tag{32}$$

$$\theta = \tan^{-1}(\dot{Y}/\dot{X}) \tag{33}$$

$$V_g = [\dot{X}^2 + \dot{Y}^2]^{1/2} \tag{34}$$

$$h = \int \frac{dh}{dt}\, dt \tag{35}$$

$$V = \int \frac{dV}{dt}\, dt \tag{36}$$

Eqs. 2 and 7 are used to calculate $\frac{dV}{dt}$ and $\frac{dh}{dt}$, respectively, for the last two integrals. The integrals above are evaluated numerically using the trapezoidal rule. Interpolation is used at the end of a segment since time is the variable of integration for the tracking part.

At each time interval the following information is printed:

T	time from entry fix (sec)
H	altitude (ft)
HDL	track heading (degrees)
HDG	aircraft heading (degrees)
X	X-position of aircraft (n.mi.)
Y	Y-position of aircraft (n.mi.)
VGKT	ground speed (kts)
VCALKT	calibrated airspeed (kts)
AM	Mach number
PHI	bank angle (degrees)
PHIR	bank angle rate (degrees/sec)
SS	heading correction factor for wind effects (degrees)
ROC	rate of climb (ft/min)
GAM	flight path inclination angle relative to the local horizontal (degrees)

3.7 Approximate Relations for Profile Descents

The equations developed above for calculating and tracking profile descents require numerical integrations for the time and distance in each segment. For some applications these calculations may require more computational effort than is desirable. Refs. 2 and 3 developed approximate relations to perform the calculations. However, their approximate expressions were found to produce significant errors in some cases. Therefore, different approximate relations are developed here.

3.7.1 Deceleration Segments. - V_0 and V_f are initial and final true airspeeds. Assume an average acceleration, then

$$\Delta t_i = \frac{\Delta V}{\left(\frac{dV}{dt}\right)_{avg}} \tag{37}$$

$$\Delta V = V_f - V_0 \tag{38}$$

where

$$\left(\frac{dV}{dt}\right)_{avg} = \frac{1}{2}\left[\left(\frac{dV}{dt}\right)_0 + \left(\frac{dV}{dt}\right)_f\right] \tag{39}$$

$$\Delta S_i = [V_{avg} + V_w \cos(\theta - \psi_w)]\, \Delta t_i \tag{40}$$

and

$$V_{avg} = \frac{1}{2}(V_0 + V_f)\,. \tag{41}$$

The accelerations $\left(\frac{dV}{dt}\right)_0$ and $\left(\frac{dV}{dt}\right)_f$ are calcualted from Eq. 2 using the aircraft data for F and C_D.

3.7.2 Descent with Constant CAS. - Since the rate of descent changes slowly and monotonically with altitude, it is sufficiently accurate to use an average value, i.e.,

$$\left(\frac{dh}{dt}\right)_{avg} = \frac{1}{2}\left[\left(\frac{dh}{dt}\right)_0 + \left(\frac{dh}{dt}\right)_f\right] \tag{42}$$

where $\left(\frac{dh}{dt}\right)_0$ and $\left(\frac{dh}{dt}\right)_f$ are calculated from Eq. 7.

Then

$$\Delta t_i = \frac{\Delta h}{\left(\frac{dh}{dt}\right)_{avg}} \tag{43}$$

and

$$\Delta S_i = [V_{avg} + V_W \cos(\theta - \psi_W)]\, \Delta t_i \quad . \quad . \qquad (44)$$

3.7.3 Descent with Constant M. - Here the rate of descent does not, in general, vary monotonically. Therefore, the average value used above is not accurate enough. It was found that using $\frac{dh}{dt}$ at 3 points and performing the integration with Simpson's rule was much more accurate. Thus

$$\Delta t_i = \int \frac{dh}{dh/dt} \approx \frac{\Delta h}{6} \left[\frac{1}{\left(\frac{dh}{dt}\right)_0} + \frac{4}{\left(\frac{dh}{dt}\right)_{mid}} + \frac{1}{\left(\frac{dh}{dt}\right)_f} \right] . \qquad (45)$$

Properties used to calculate $\left(\frac{dh}{dt}\right)_{mid}$ are calculated from V_{avg} and h_{avg}. Then

$$\Delta S_i = [V_{avg} + V_W \cos(\theta - \psi_W)]\, \Delta t_i \quad . \qquad (46)$$

3.7.4 Approximate Airspeed-Mach Number Relations. - Ref. 2 gives approximate, yet simple, equations to relate true airspeed to Mach number and calibrated airspeed. They are given below.

$$V(kts) = M\,(661 - 2.43 \times 10^{-3}\, h) \qquad (47)$$

$$V(kts) = \frac{CAS}{1 - 0.12 \times 10^{-4}\, h} \quad . \qquad (48)$$

The cross-over altitude where M_d and CAS_d are prescribed can be determined by equating the right sides of the two equations above and solving for the altitude. These approximate relations are reasonably accurate for altitudes below 36,089 ft, and for calibrated airspeed between 210 and 350 kts.

The equations above can be differentiated to obtain dV/dh for the rate of climb at constant Mach number and constant calibrated airspeed. These relations are much simpler than Eqs. C-1 through C-4 for dV/dh given in Appendix C.

3.7.5 Approximation to Effect of Weight. - The effect of weight on the time can be determined from simple relations if the weight effect on the drag coefficient is neglected. For all segments, except Segment 4, it follows from Eqs. 13, 15, and 17 that

$$\Delta t_{i_{new}} = \Delta t_{i_{old}} \frac{W_{new}}{W_{old}} \quad (i = 1, 2, 3, \text{and } 5) \tag{49}$$

whereas for Segment 4

$$\Delta t_{4_{new}} = \Delta t_{4_{old}} \frac{W_{new}}{W_{old}} + \frac{\Delta S_{TOT}}{V_4} \left(1 - \frac{W_{new}}{W_{old}} \right). \tag{50}$$

Thus the total time is approximately

$$\Delta t_{TOT_{new}} = \Delta t_{TOT_{old}} \frac{W_{new}}{W_{old}} + \frac{\Delta S_{TOT}}{V_4} \left(1 - \frac{W_{new}}{W_{old}} \right). \tag{51}$$

If $\frac{\Delta S_{TOT}}{V_4} \approx \Delta t_{TOT_{old}}$, then the weight changes have only a small effect on the time required to perform the profile descent.

4.0 RESULTS AND DISCUSSION

4.1 Example Profile Descent

To illustrate the application of the computer algorithm, a profile descent was calculated for the NASA B-737 aircraft using the following input data:

Table 4-1. Input data for B-737 profile descent.

W	=	87,500 lb	VCMF	=	250 kts
S	=	940 ft^2	AMC	=	0.78
TO	=	519° R	AMMAX	=	0.78
PO1	=	2116.2 lb/ft^2	AMMIN	=	0.60
HC	=	35,000 ft	VCMX	=	340 kts
HFMAX	=	23,000 ft	VCMN	=	250 kts
HFMIN	=	19,500 ft	DSTOT	=	75 n.mi.
HAP	=	9,000 ft	HDGTRK	=	238°
DAP	=	10 n.mi.	TREQ	=	700 sec
DSC	=	5 n.mi.	KSEQ	=	0
VCAP	=	170 kts	NO WIND		
VCSC	=	210 kts			

The B-737 idle thrust and drag data were taken from Ref. 1 and are shown on Figs. 4-1 and 4-2. Fuel flow-rate data was also taken from Ref. 1.

A profile descent is required to take the aircraft from the entry fix at cruise conditions h_c = 35,000 ft and M_c = 0.78 down to a metering fix which has an altitude window $h_{mf,min} \leq h_{mf} \leq h_{mf,max}$ and has a required speed of CAS_{mf} = 250 kts. The distance between the entry fix and the metering fix is DSTOT = 75 n.mi. and the time required to perform this portion of the profile descent is TREQ = 700 sec.

The remaining portion of the profile descent is between the metering fix and the aim point. The aim point is specified to be 10 n.mi. from the metering fix and the speed and altitude there are CAS_{ap} = 170 kts and h_{ap} = 9,000 ft. A speed control segment is specified to begin at 5 n.mi. from the metering fix with CAS_{sc} = 210 kts. The various segments are shown on Figure 1-1.

The computer algorithm calculates the segments between the metering

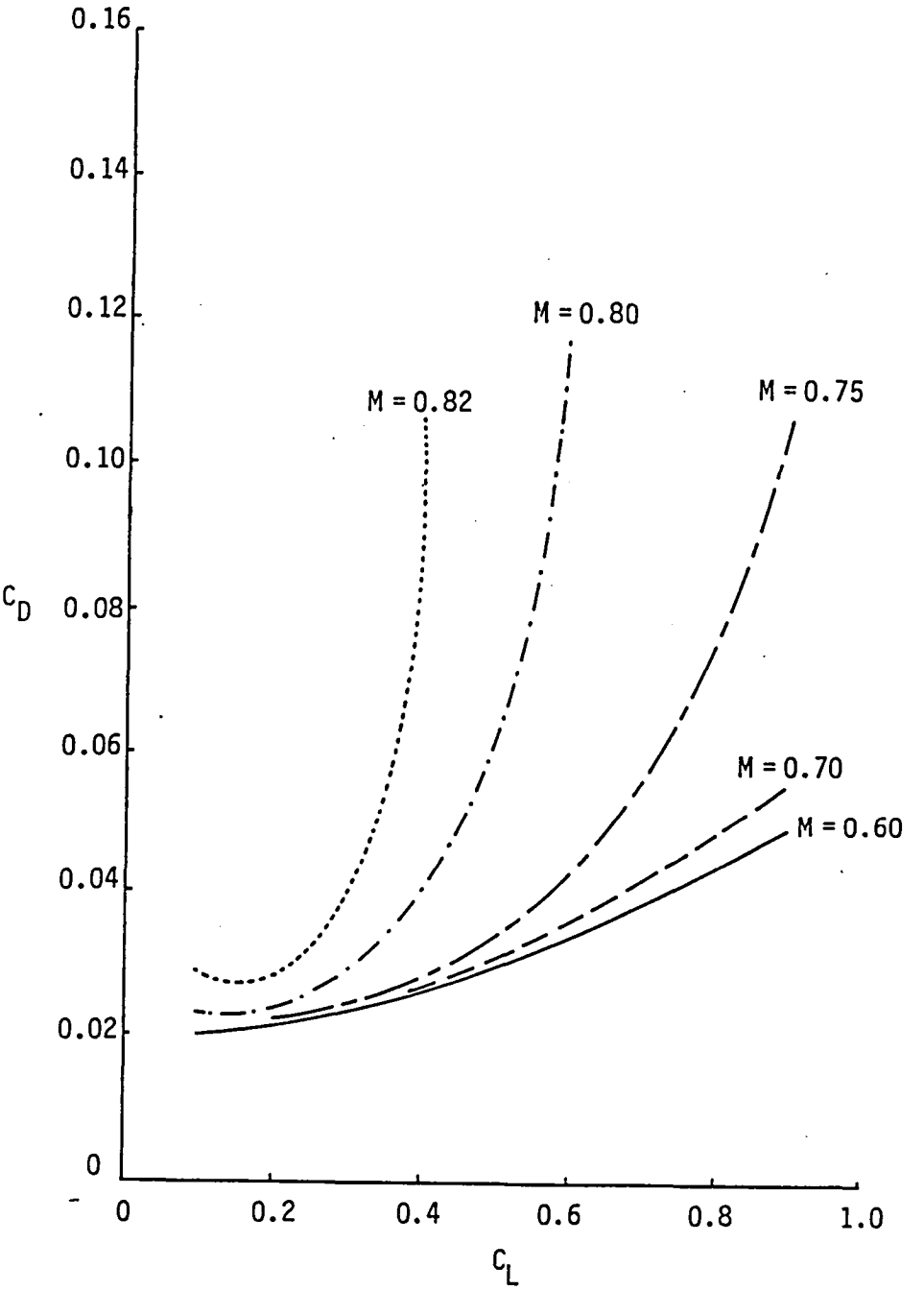

Figure 4-1. B-737 drag coefficient.

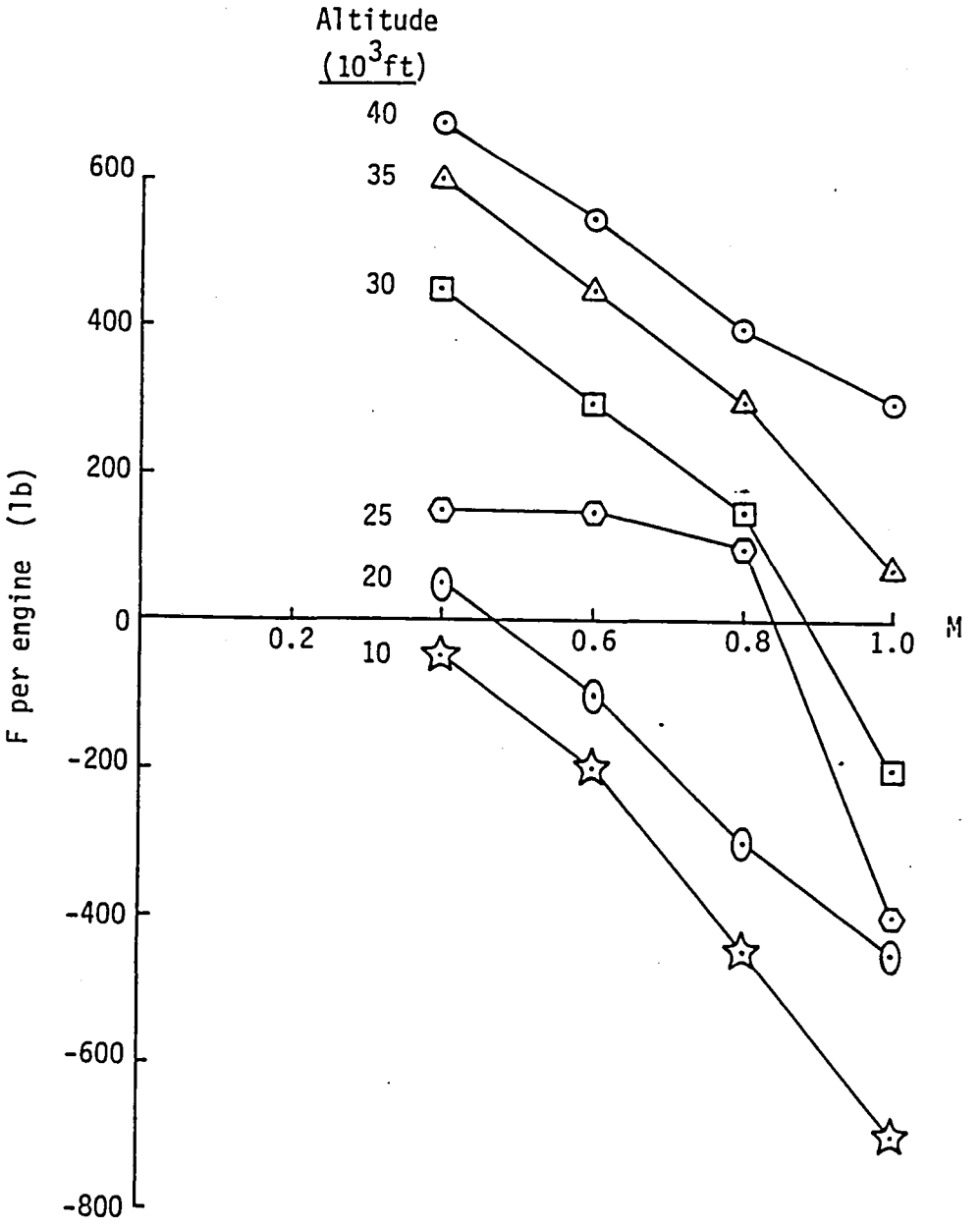

Figure 4-2. B-737 idle thrust.

fix and the aim point first so that the altitude at the metering fix can be determined. From the conditions specified at the metering fix and aim point, it was found that the ground distance between these two positions must lie within the range

$$43.88 \text{ n.mi.} \leq \text{DAP} \leq 57.87 \text{ n.mi.}$$

However, the input value of DAP was 10 n.mi. Since this value is less than the minimum range, the computer program changes the input value of DAP to the minimum value of 43.88 n.mi. which gives the altitude at the metering fix to be the minimum value of 19,500 ft. The distance and time for each segment of this region are given below.

Table 4-2. Distance and time for segments between metering fix and aim point.

	Segment				
	1A	2A	3A	4A	Total
ΔS_i (n.mi.)	35.54	3.34	1.12	3.88	43.88
Δt_i (sec)	606.8	50.4	14.3	45.5	717.0

The altitude for segment 2A (speed control segment) was calculated to be 19,150 ft.

With the altitude at the metering fix set at 19,500 ft, the computer algorithm determined iteratively the combination

$$M_d/CAS_d = 0.67/263.7 \text{ kts}$$

for the descent segments between the entry fix and the metering fix. The cross-over altitude corresponding to these values was

$$h_x = 27{,}702 \text{ ft.}$$

The distance, time, and fuel consumed for each segment are given in Table 4-3.

Table 4-3. Distance, time and fuel consumed for segments between entry fix and metering fix.

	SEGMENT					TOTAL
	1	2	3	4	5	
ΔS_i (n.mi.)	1.35	25.00	19.24	23.13	6.27	74.99
Δt_i (sec)	14.3	240.6	176.5	215.5	54.2	701.1
$\Delta w_{f,i}$ (lb)	4.4	72.3	53.0	247.1	16.3	393.1

Note that the total time required is 701.1 sec rather than the input value of 700 sec because the convergence criterion for the iterative procedure is $\pm$ 3 sec. Of the 393 lb of fuel consumed, the largest amount occurred in Segment 4. Since this is a constant speed segment, engine thrust must be greater than idle thrust and, hence, the rate of fuel consumption is higher than for idle thrust.

4.1.1 Influence Parameters. - For the profile descent calculated above between the entry fix and the metering fix, the following influence parameters were calculated:

Table 4-4. Change in parameters to increase time one second.

PARAMETER	CHANGE REQUIRED TO INCREASE Δt_{req} ONE SEC
h_{mf}	-322 ft
M_d	-0.0016
CAS_d	-2.3 kts
h_c	817 ft
M_c	-0.018
ΔS_{TOT}	0.11 n.mi.
W	25,636 lb

These influence parameters were used to estimate the uncertainty in Δt_{TOT}, and the results are given below.

Table 4-5. Effect of uncertainty in parameters on time.

PARAMETERS	ESTIMATED UNCERTAINTY	EFFECT ON Δt_{TOT} (sec)
h_{mf}	$\pm$200 ft	$\pm$0.62
M_d	$\pm$0.01	$\pm$6.18
CAS_d	$\pm$3 kts	$\pm$1.30
h_c	$\pm$500 ft	$\pm$0.61
M_c	$\pm$0.01	$\pm$0.54
ΔS_{TOT}	$\pm$0.2 n.mi.	$\pm$1.86
W	$\pm$5,000 lb	$\pm$0.20
	WORST CASE TOTAL	$\pm$11.31 sec

This table shows that the uncertainty in M_d has the largest effect ($\pm$6.18 sec) on the total time (701 sec), whereas the weight has the least effect ($\pm$0.20 sec). The approximate equations given by Eqs. 49 and 50 showed that Δt_i increased with weight for all segments except Segment 4 which decreased with an increase in weight. Thus compensating effects cause the overall effect of weight to be small for this example.

An investigation was also made to determine the range of linearity for the effect of influence parameters on the total time required for the profile descent described above. As long as $\Delta S_4 > 0$, changes in ΔS_{TOT} affect Segment 4 only; and since the speed is constant in that segment, changes in ΔS_{TOT} influence Δt_{TOT} linearly. Fig. 4-3 shows the influence of weight and cruise altitude, separately, on the total time. Changes in cruise altitude of $\pm$1,000 ft produced changes in total time of less than 1.2 sec, and the variation is nearly linear over this range. The influence

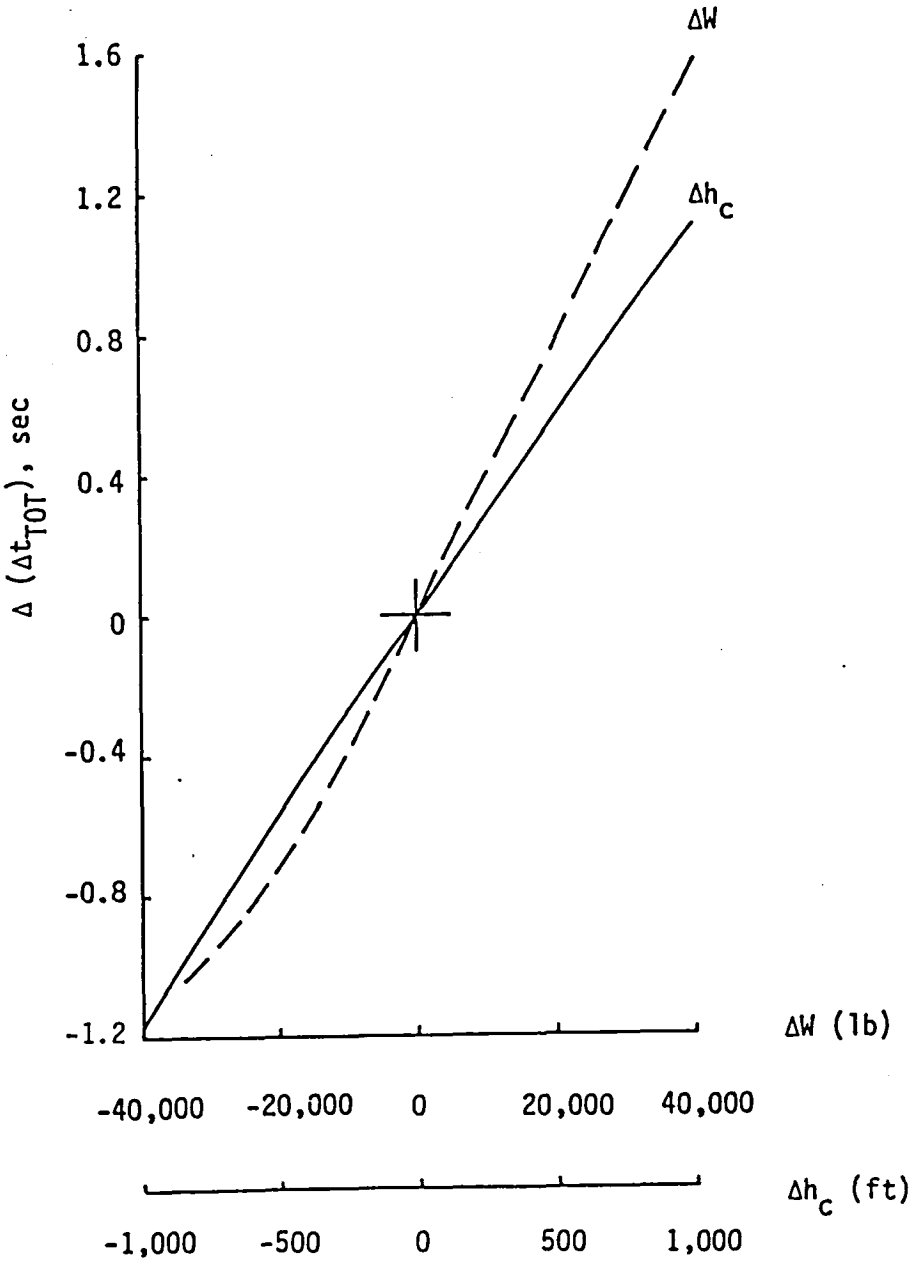

Figure 4-3. Influence of changes in weight and cruise altitude on time.

of weight was nearly linear for weight changes up to ±10,000 lb. However, weight changes of ±40,000 lb (out of 87,500 lb) produced changes in total time of less than 1.6 sec. Fig. 4-4 illustrates the influence of descent calibrated airspeed and metering-fix altitude on total time. The curves are nearly linear for ΔCAS_d within ±2.5 kts and Δh_{mf} within ±500 ft. Changes in total time for these two parameters are greater than those in Fig. 4-3. Fig. 4-5 shows the influence of cruise and descent Mach numbers on the total time. Changes in cruise Mach number within ±0.02 produced changes in total time which are nearly linear. However, changes of ±0.08 in M_c changed the total time less than 4 sec. As already mentioned, relatively small changes in descent Mach number produce large changes in total time. For descent Mach number changes of ±0.02, time changes greater than 12 sec were calculated, and the variation is nearly linear over this range.

4.1.2 Span of Control. - In the previous example, one combination of M_d/CAS_d was determined which would allow the aircraft to fly from the entry fix to the metering fix for the specified end conditions. Actually, there are an infinite number of combinations of M_d/CAS_d which will accomplish this objective. This can be observed in Fig. 4-6 which shows the span of control for the B-737. In this figure, the speeds and altitudes given earlier were used for the entry and metering fixes and the total distance ΔS_{tot} was fixed at 76.05 n.mi. The two-gradient wind profile shown on Fig. 4-7 for the Denver airport was used and the ground heading was $\theta = 238°$. Note that the wind angle ψ_W given in Fig. 4-7 is 180° from the wind direction, and for this example it gives the aircraft side- and tail-wind components. Results are given for Segments 4 and 5 the same as described earlier, and with these two segments reversed. The descent Mach, M_d, was varied from the minimum to the maximum value, and the descent calibrated airspeed, CAS_d, was varied over the allowable range. It was found that some combinations of M_d/CAS_d produced cross-over altitudes, h_x, below h_{mf} or greater than h_c. When this occured, the computer algorithm changes CAS_d to make $h_x = h_{mf}$ when $h_x < h_{mf}$ or make $h_x = h_c$ when $h_x > h_c$. These changes are shown in Fig. 4-8.

Fig. 4-6 shows that a greater span of control is available when Segment 4 is the constant speed segment and Segment 5 is the deceleration

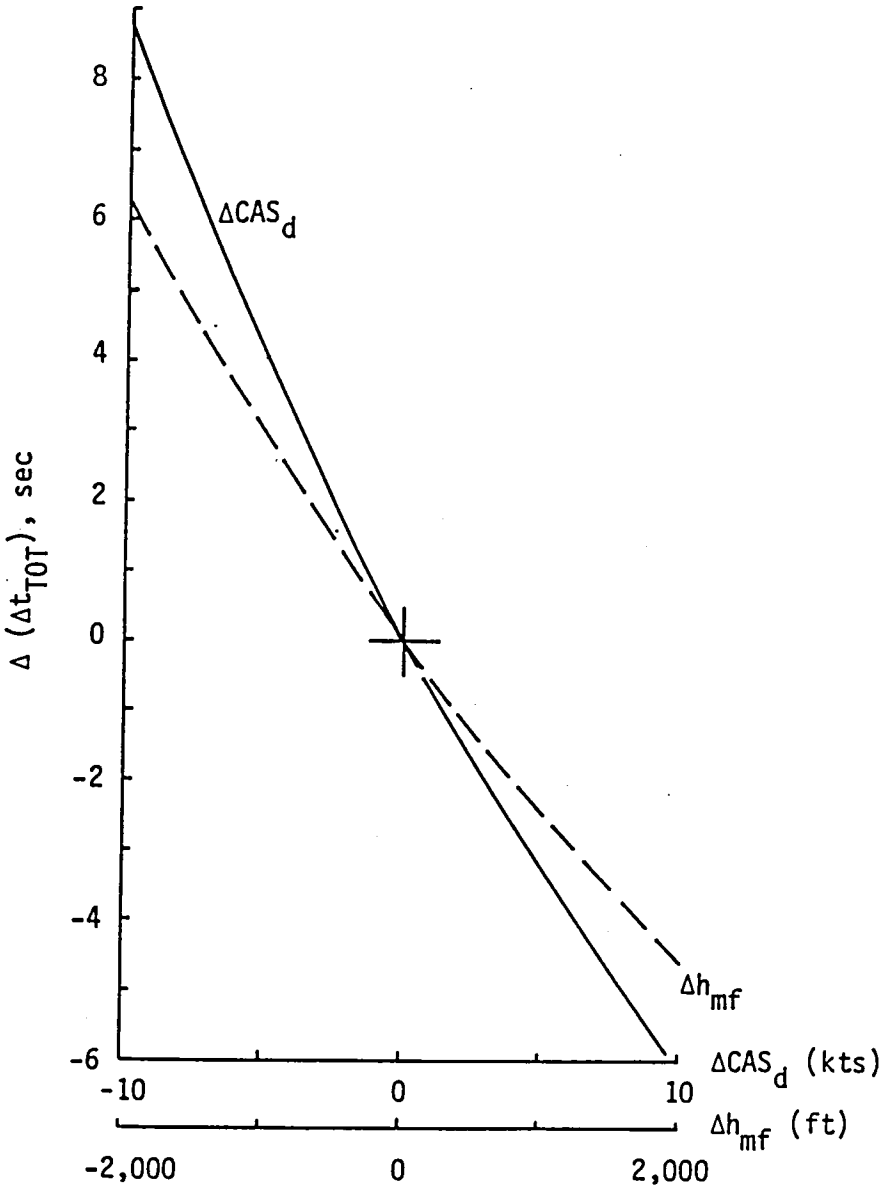

Figure 4-4. Influence of changes in calibrated airspeed and metering-fix altitude on time.

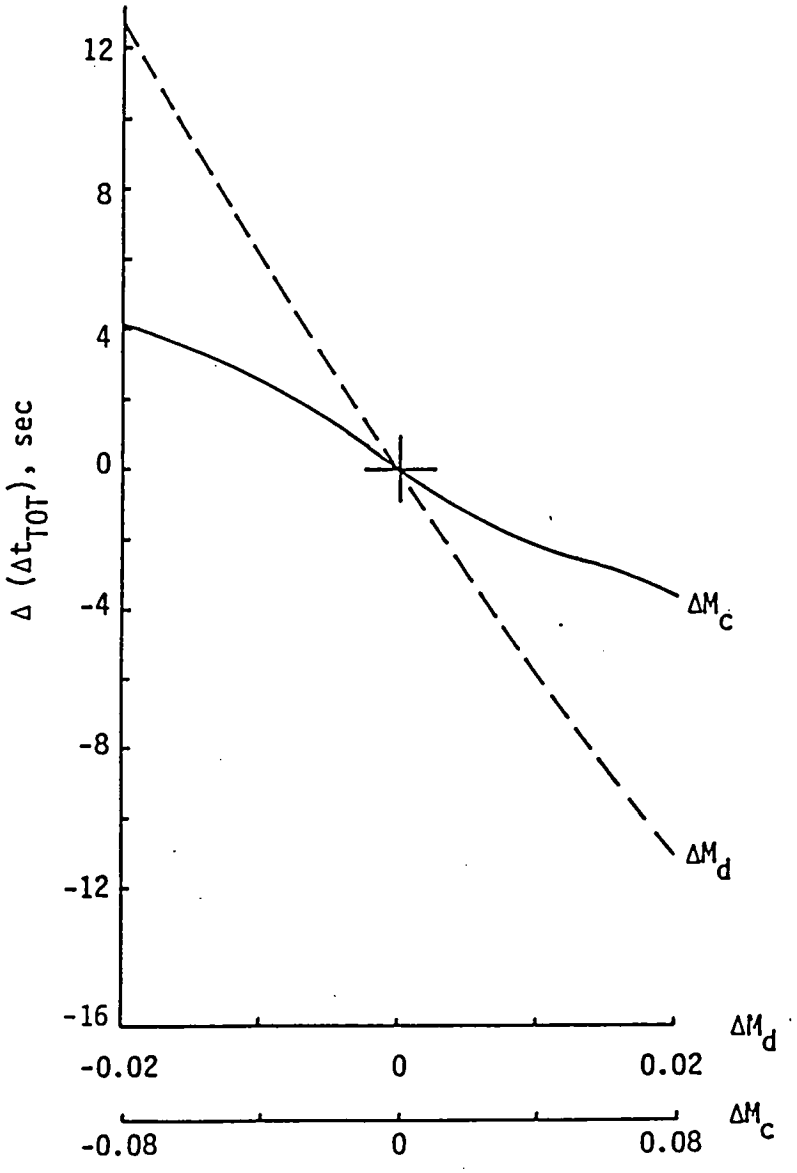

Figure 4-5. Influence of changes in cruise and descent Mach numbers on time.

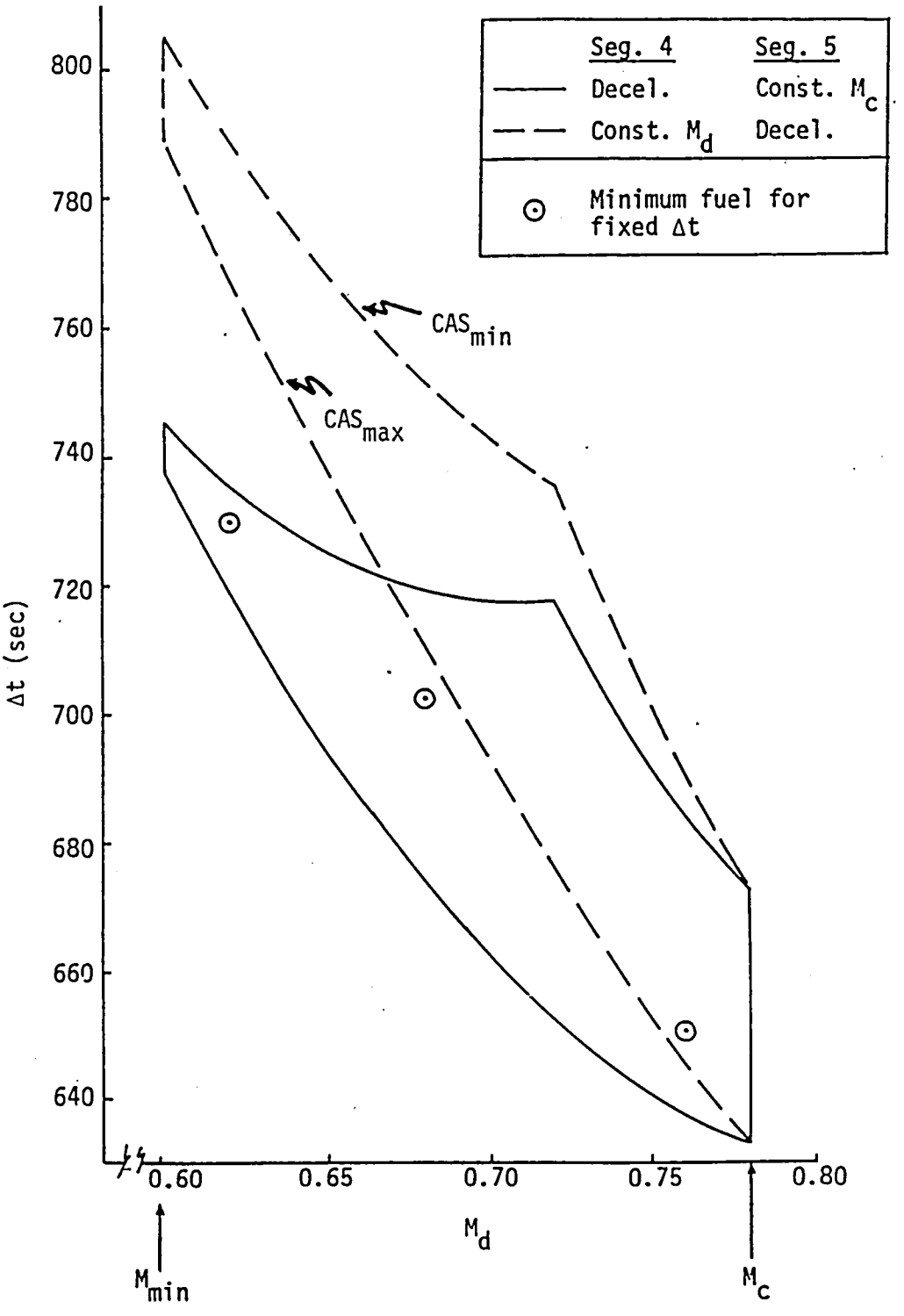

Figure 4-6. Control span for B-737 profile descent.

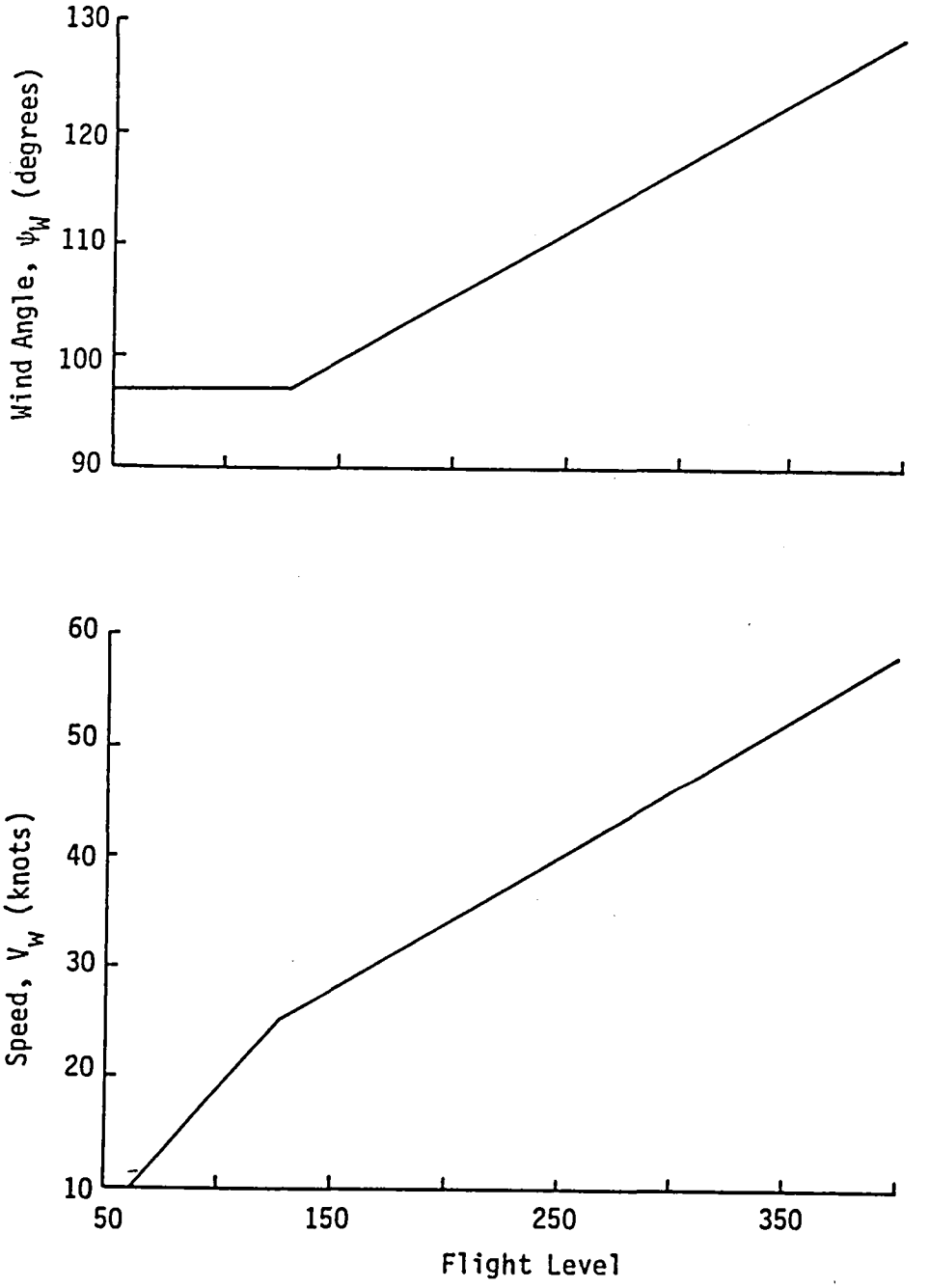

Figure 4-7. Wind model for Denver airport.

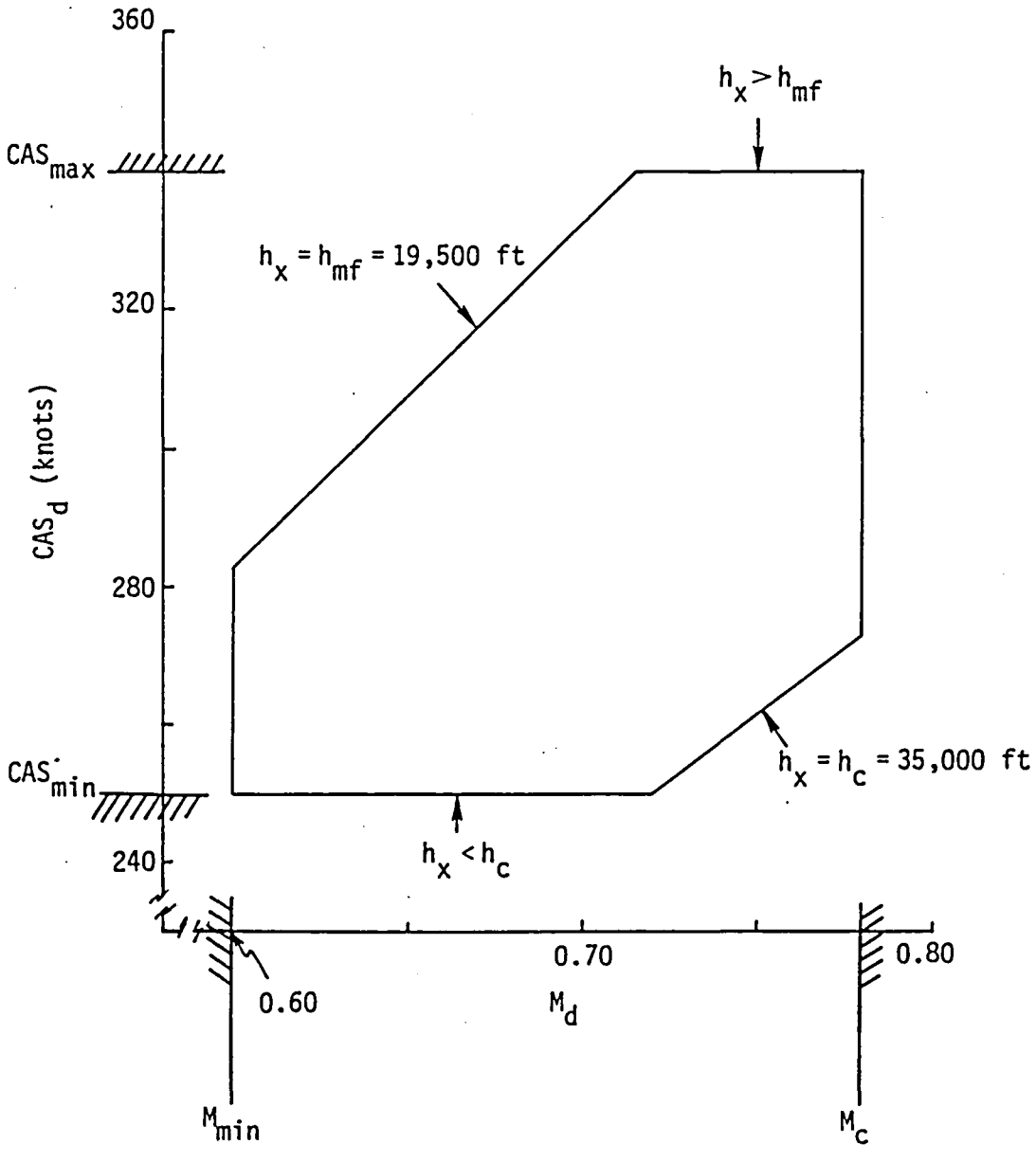

Figure 4-8. Limits of M_d/CAS_d for profile descent.

segment. Refs. 2 and 3 had these two segments reversed. The two envelopes merge when $M_d = M_c$ because the deceleration segment has zero length. For a specified value of Δt_{TOT}, the envelopes give the range of M_d which will produce the desired profile descent. The corresponding range of CAS_d is shown on Fig. 4-9 for Segment 4 the deceleration segment and Segment 5 at constant speed.

Fig. 4-10 gives the envelopes of control spans for ΔS_{TOT} = 50, 75, and 100 n.mi. with no wind. The envelopes for 75 and 100 n.mi. are similar, but displaced. However, the envelope for 50 n.mi. is much smaller because when $M_d < 0.77$ a profile descent is not possible for the prescribed end conditions.

4.1.3 Effects of Wind and Non-Standard Day. - Wind can have a significant effect on the time required to perform a profile descent because it changes the ground speed. Consider the wind speed (V_w) model given in Fig. 4-7 for the Denver airport. Calculations were performed for the B-737 using this wind speed, but the wind direction was for a head wind, side wind, and tail wind on a standard day. The envelopes of spans of control are shown on Fig. 4-11 for a distance between the entry fix and metering fix of 75 n.mi. The influence of the wind is even greater when this distance is increased. Note that with the approximations used for Eq. 22, the side wind has no effect on the ground speed; thus the calculated profile descent is the same as that with no wind.

It was found that non-standard atmospheric temperatures have a significant effect on calculated profile descents. For the B-737 aircraft approaching the Denver airport, profile descents were calculated for sea-level temperatures of 59° F (standard day) and 80° F (hot day). Again, the distance between the entry and metering fixes was 76 n.mi., a required time of 702 sec and a descent Mach number of M_d = 0.67 were specified for each case. In order to satisfy the end conditions, the CAS_d had to be 290 kts for the standard day and 267 kts for the hot day. The results are given in Table 4-6.

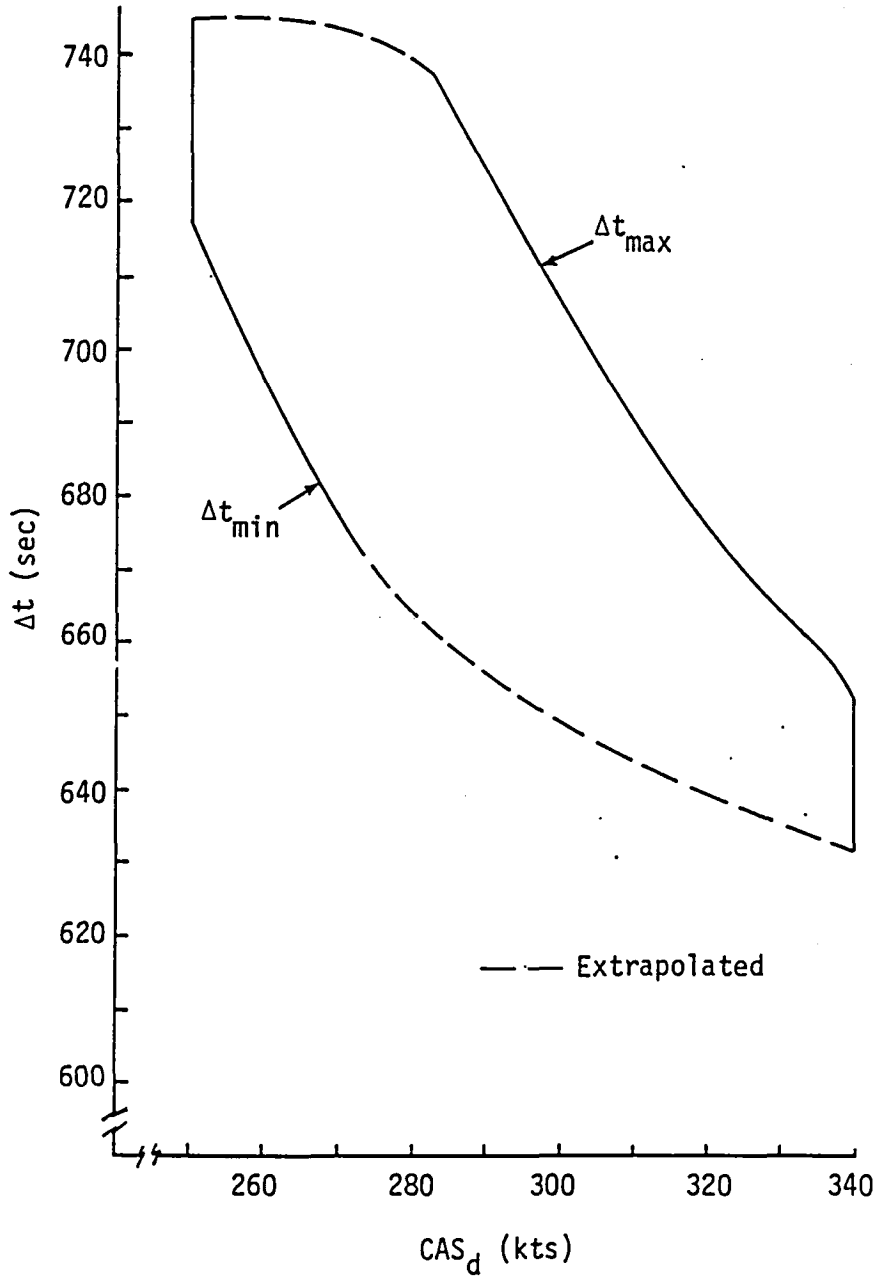

Figure 4-9. Control span for specified CAS_d.

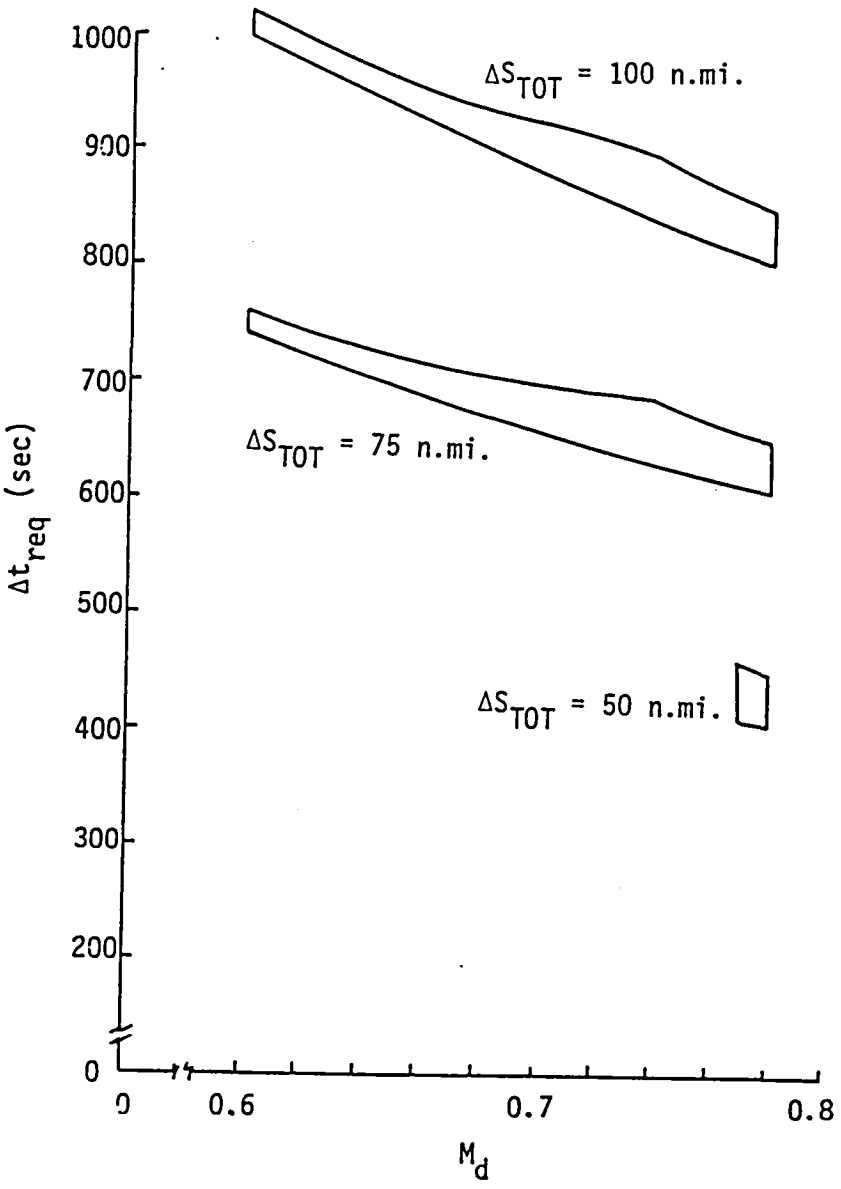

Figure 4-10. Effect of distance on control span for no wind.

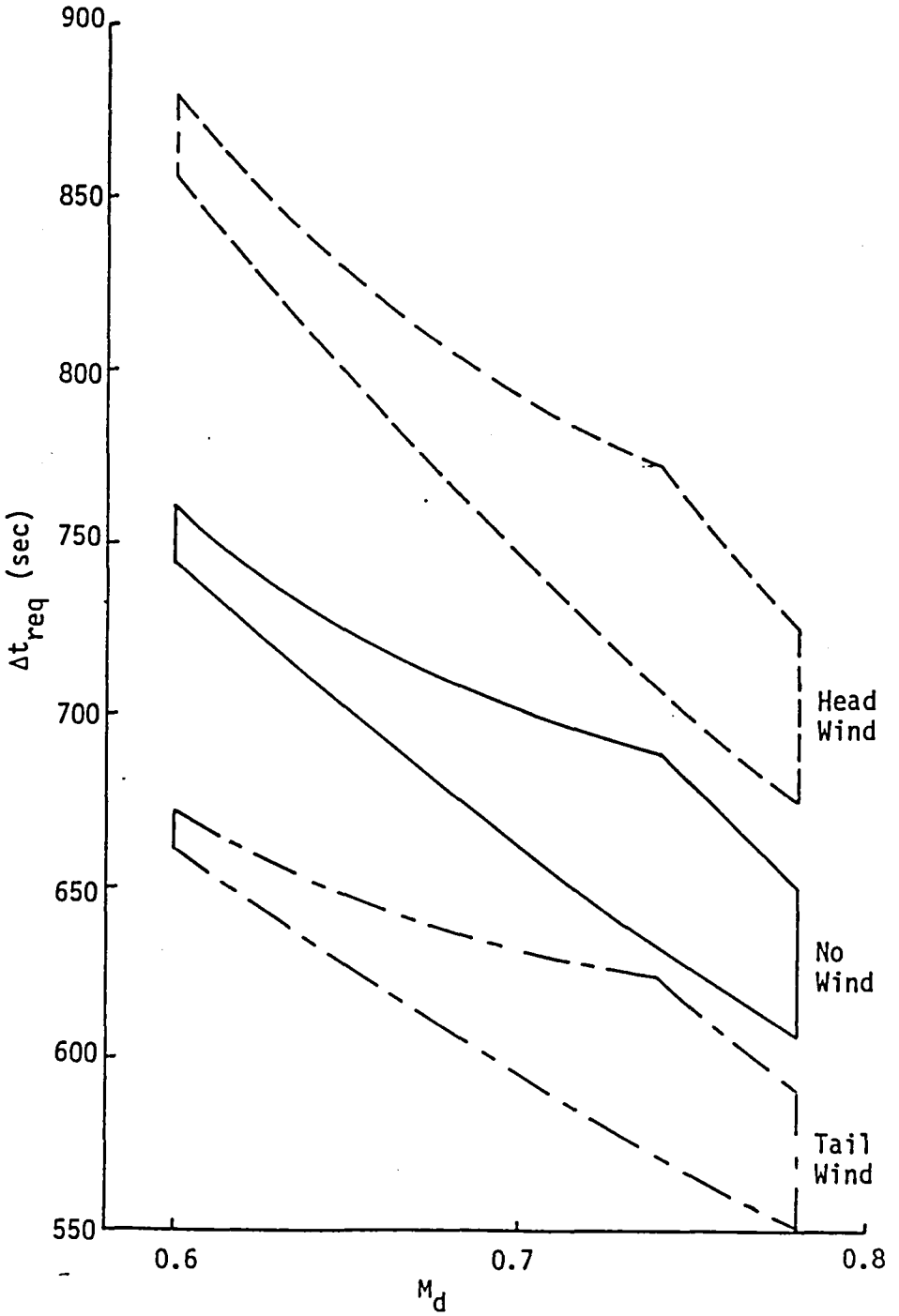

Figure 4-11. Effect of wind on control span.

Table 4-6. Effect of hot day on profile descent.

SEGMENT NUMBER	STANDARD DAY		HOT DAY	
	Δt_i (sec)	ΔS_i (n.mi.)	Δt_i (sec)	ΔS_i (n.mi.)
1	39.7	3.70	13.2	1.18
2	89.7	9.28	278.0	27.38
3	271.0	28.03	140.7	14.79
4	54.8	5.91	55.0	6.20
5	244.9	29.10	216.9	26.49
TOTAL	700.1	76.02	703.8	76.04

Note the differences in the individual segments. It is also of interest to note that the fuel consumed for the standard-day profile descent was 499 lb, whereas it was 467 lb for the hot day. These results show that the non-standard atmospheric effects are important and should be included in the calculations.

4.1.4 Optimal M_d/CAS_d Combination for Minimum Fuel. - For fixed end conditions, there are normally an infinite number of M_d/CAS_d combinations which could be used to fly the profile descent between the entry and metering fixes. Ref. 7 discusses optimal values of CAS_d for minimum fuel consumed when the entire descent is performed at constant calibrated airspeed. An investigation was made here to determine the optimal combination of M_d/CAS_d which requires minimum fuel. The computer algorithm calculates the fuel consumed for each profile descent possible for increments in M_d of 0.01 for $M_{min} \leq M_d \leq M_{max}$. For each value of M_d there is only one value of CAS_d that will satisfy the required end conditions. Then the computer program determines the M_d/CAS_d combination which requires minimum fuel consumption. Results for the B-737 flying the profile descent described above with ΔS_{TOT} = 75 n.mi. and no wind are shown on Fig. 4-12. This figure shows that the differences in total fuel consumption are small,

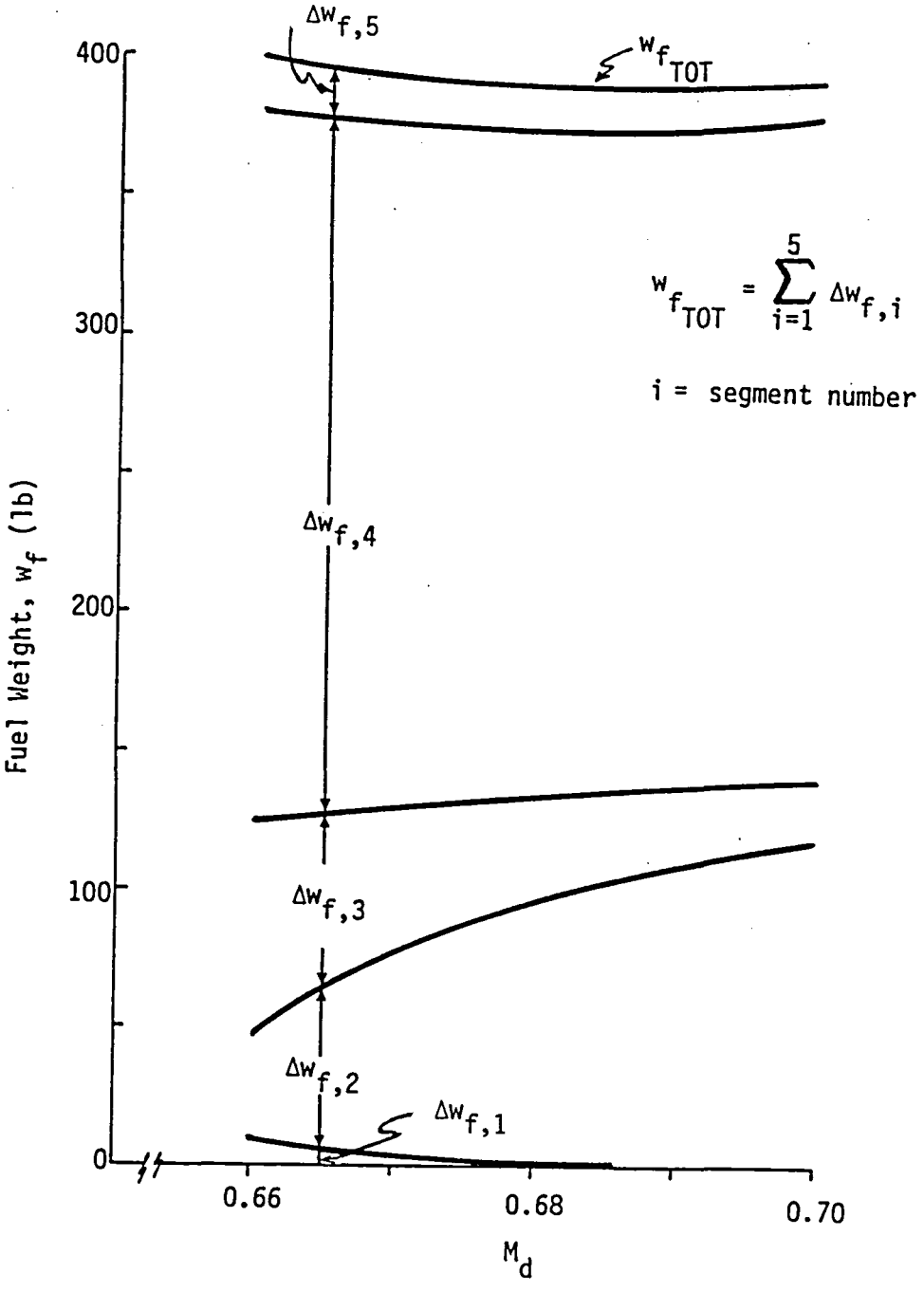

Figure 4-12. Effect of M_d on fuel consumed.

and hence some other criteria would probably be more important in the determination of the M_d/CAS_d combination. An alternative criterion used in the computer program is the determination of the combination of M_d/CAS_d for which the difference between the desired metering-fix arrival time and minimum arrival time is 30% of the span of time control at that value of M_d. The 30% proportionality constant was chosen based on the assumptions that delay, rather than advancement, is prevalent. This scheme allows some flexibility to compensate for deviations from the predicted profile and/or subsequent changes in the desired metering-fix arrival time generated by terminal dynamics. Obviously, this flexibility decreases as the aircraft approaches the metering fix.

4.1.5 Delay Capabilities. - Due to constantly changing conditions near an airport, it is necessary to know how much time a flight might be delayed at some point in the profile descent and still fly a clean configuration/idle thrust trajectory to the metering fix. Calculations were performed for the B-737 approaching the Denver airport to determine the maximum delay capability at every position in the profile descent. At any position before or in the profile descent this requires changes in the remaining segments that will consume the maximum time to arrive at the metering fix at the prescribed altitude and calibrated airspeed there. The difference between the maximum time and the time required for the original profile descent is the maximum delay capability at that position. Fig. 4-13 shows the maximum delay capability as a function of time from the metering fix. Prior to arriving at the entry fix, a delay could be achieved by initiating the profile descent before the original entry fix. For the profile descent planned originally in Fig. 4-13, a maximum delay of 133 sec is possible when 800 sec from the metering fix. While in Segment 5, a maximum delay of 103 sec is available and this value does not change until Segment 4 begins because the deceleration could be continued beyond the planned end-of Segment 5. In Segment 4, the constant speed segment, the maximum delay capability decreases rapidly to virtually none at the end of Segment 4.

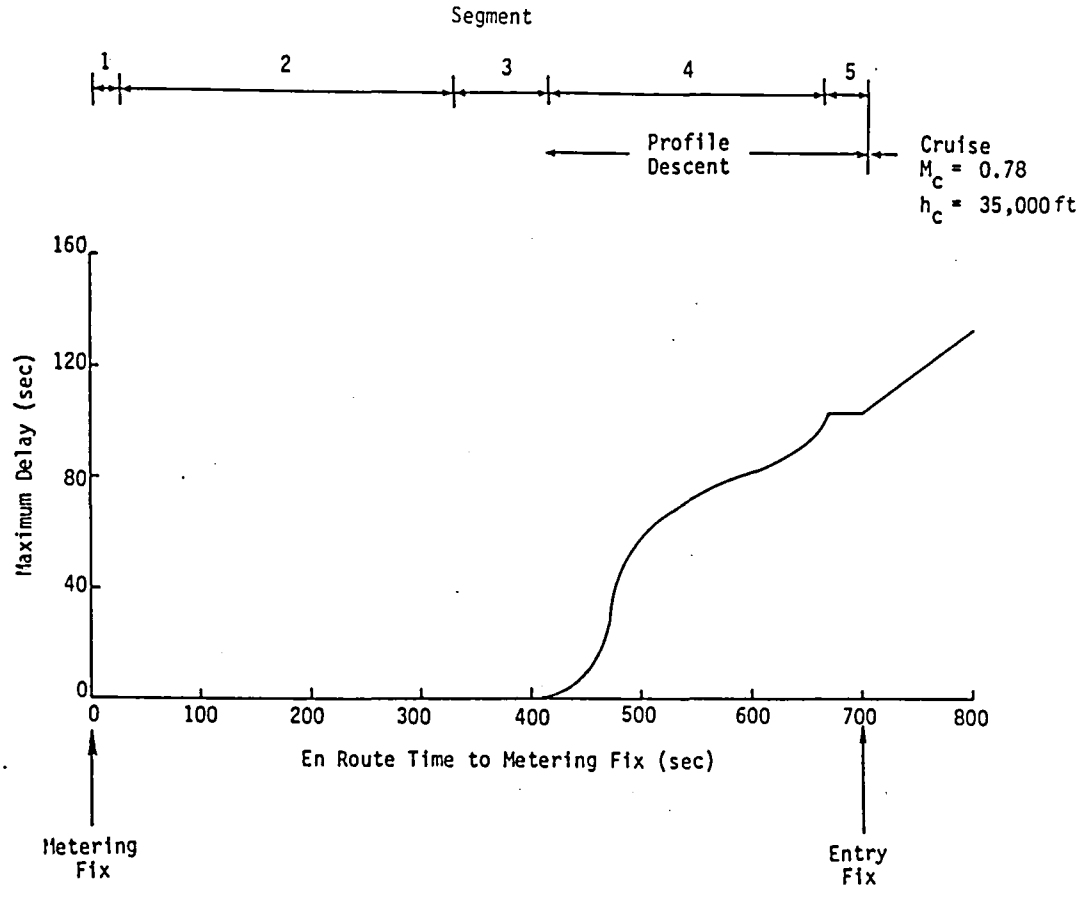

Figure 4-13. Delay capability in profile descent.

It was found that the maximum delay capability available after the descent was begun (after Segment 4) was very small. This fact, coupled with the additional work load on the pilot to make changes during the descent, led to the decision to restrict profile changes to those segments before the descent segments.

4.1.6 Comparison with Flight Simulator. - A profile descent was flown on the NASA/LRC B-737 TCV simulator and the results were compared with the computational results from the computer algorithm described herein. In order to compare with the simulator time and distance for each segment, the profile descent was calculated from the conditions listed below:

(1) Cruise conditions of W = 85,000 lb, h = 34,000 ft, M = 0.78
(2) Descend with M_d/CAS_d = 0.78/280 kts to h = 10,000 ft
(3) Decelerate from CAS = 280 kts to 250 kts at 10,000 ft
(4) Descend to 6,000 ft at 250 kts
(5) Decelerate from 250 kts to 210 kts at 6,000 ft

The idle thrust used in the simulator was different from that shown in Fig. 4-2. Therefore, the idle thrust used in the calculations was changed to duplicate that in the simulator. The results are shown in the table below.

Table 4-7. Comparison of calculated and flight simulator profile descent.

SEGMENT	Δt_{sim}(sec)	Δt_{cal}(sec)	ΔS_{sim}(ft)	ΔS_{cal}(ft)
Descent at M_d = 0.78	25	24.6	18,760	18,814
Descent at CAS_d = 280 kts	587	598.6	379,368	387,145
Deceleration at 10,000 ft	27	26.3	13,772	13,535
Descent at CAS = 250 kts	136	148.8	64,646	70,466
Deceleration at 6,000 ft	51	39.9	21,273	16,857
TOTAL	826	838.2	497,819	506,817

The calculated total time and distance was within 2% of the simulator results. An investigation of each segment shows that the calculated results for the descent at M_d = 0.78 and deceleration at 10,000 ft segments compare well with the corresponding results from the simulator. However, the descent segments at constant CAS and the deceleration segment at 6,000 ft did not compare nearly so well with the simulator results. Part of the differences noted for the two descent segments could be attributed to the transition at the beginning and end of these segments. The computer algorithm assumes instant transition. The larger part of the differences between calculated results and simulator results can be traced to pilot technique which produces speeds and flight path angles different from the prescribed values.

Of particular note is the effect of flight path angle on the deceleration segment at 6,000 ft. The simulator results show $\gamma = 0.44°$ at the beginning and $\gamma = -1.57°$ at the end of this segment, whereas the desired path is $\gamma = 0$. Eq. 1 gives the deceleration as

$$\frac{dV}{dt} = \frac{g}{W}(F-D) - g \sin \gamma .$$

Normally the last term on the right would be small compared to the first term for small values of γ. However, the first term is small here because of idle thrust and the relatively low speed (250 kts CAS). The table below shows the magnitude of these two terms for the beginning and end of this segment.

Table 4-8. Comparison of values for deceleration.

POSITION	γ	$g(F-D)/W$	$-g \sin \gamma$	dV/dt
beginning	-0.44°	-1.22 kt/sec	-0.15 kt/sec	-1.37 kt/sec
end	-1.57°	-1.08 kt/sec	+0.52 kt/sec	-0.56 kt/sec

Note that the flight path angle at the end of this segment produces an acceleration (0.52 kt/sec) which is nearly the same magnitude as the deceleration (-0.56 kt/sec). If the results above are corrected for $\gamma = 0$, the simulator results for time and distance in this last segment are very close to the value calculated here. Depending on pilot technique, it is possible for the regions of positive γ to compensate for the regions of negative γ over a deceleration segment; thus producing the same effect as $\gamma = 0$ throughout the segment.

4.2 Profile Descent for Heavy-Class of Aircraft

Previous results were for the B-737 airplane. In this section a profile descent is described for an aircraft whose characteristics are similar to the B-747 aircraft. The pertinent input data to the computer program are given below:

Table 4-9. Input data for heavy-class aircraft profile descent.

W	=	500,000 lb
S	=	5,500 ft^2
TO	=	519° R
PO1	=	2116.2 lb/ft^2
HC	=	40,000 ft
HFMAX	=	23,000 ft
HFMIN	=	19,000 ft
HAP	=	9,000 ft
DAP	=	36.7 n.mi.
DSC	=	21.2 n.mi.
VCAP	=	170 kts
VCSC	=	210 kts
VCMF	=	250 kts
AMC	=	0.85
DSTOT	=	76.049 n.mi.
TREQ	=	675 sec
KSEQ	=	0

NO WIND

For this case, the distance from the entry fix to the metering fix is about the same as that for one of the B-737 cases (76.049 n.mi.). The cruise conditions at the entry fix are M_c = 0.85 and h_c = 40,000 ft. A profile descent was required to fly the aircraft from the entry fix to the metering fix, where the altitude window is 19,000 ft to 23,000 ft and the calibrated airspeed is 250 kts, and arrive there in 675 sec. The aim point is 36.7 n.mi. from the metering fix at an altitude of 9,000 ft and the speed there is 170 kts. A speed control segment is allowed with a calibrated airspeed of 210 kts.

From the conditions specified at the metering fix and aim point, the computer algorithm calculated a metering-fix altitude of 22,753 ft. Then M_d/CAS_d = 0.69/296 kts was determined as one combination which would allow the aircraft to arrive at the metering fix at the prescribed time of 675 sec. The additional time required to fly from the metering fix to the aim point was 526 sec.

Results for this profile descent are shown graphically in Fig. 4-14. This figure shows the rate of descent, descent angle, and altitude as a function of time measured from the entry fix. The rate of descent varies nearly linearly with time (and hence altitude) in those segments where descent is performed at constant calibrated airspeed. However, the rate of descent did not change monotonically with time or altitude for Segment 3 (constant Mach descent). These characteristics for the rate of descent were found to hold for other aircraft as well. Therefore, the approximate relations given earlier by Eqs. 43 and 45 are justified. It is also observed that $|\gamma| < 6°$ and $|d\gamma/dt|$ is small which verifies the approximations used in Eq. 9. Although γ and $d\gamma/dt$ are discontinuous at the end points of descent segments, it was observed in the comparison with the flight simulator that the effect of these approximations on the arrival times at the metering fix and aim point are small. Fig. 4-14 also indicates that flight times for a larger aircraft like the B-747 are comparable to those of the B-737 for profile descents.

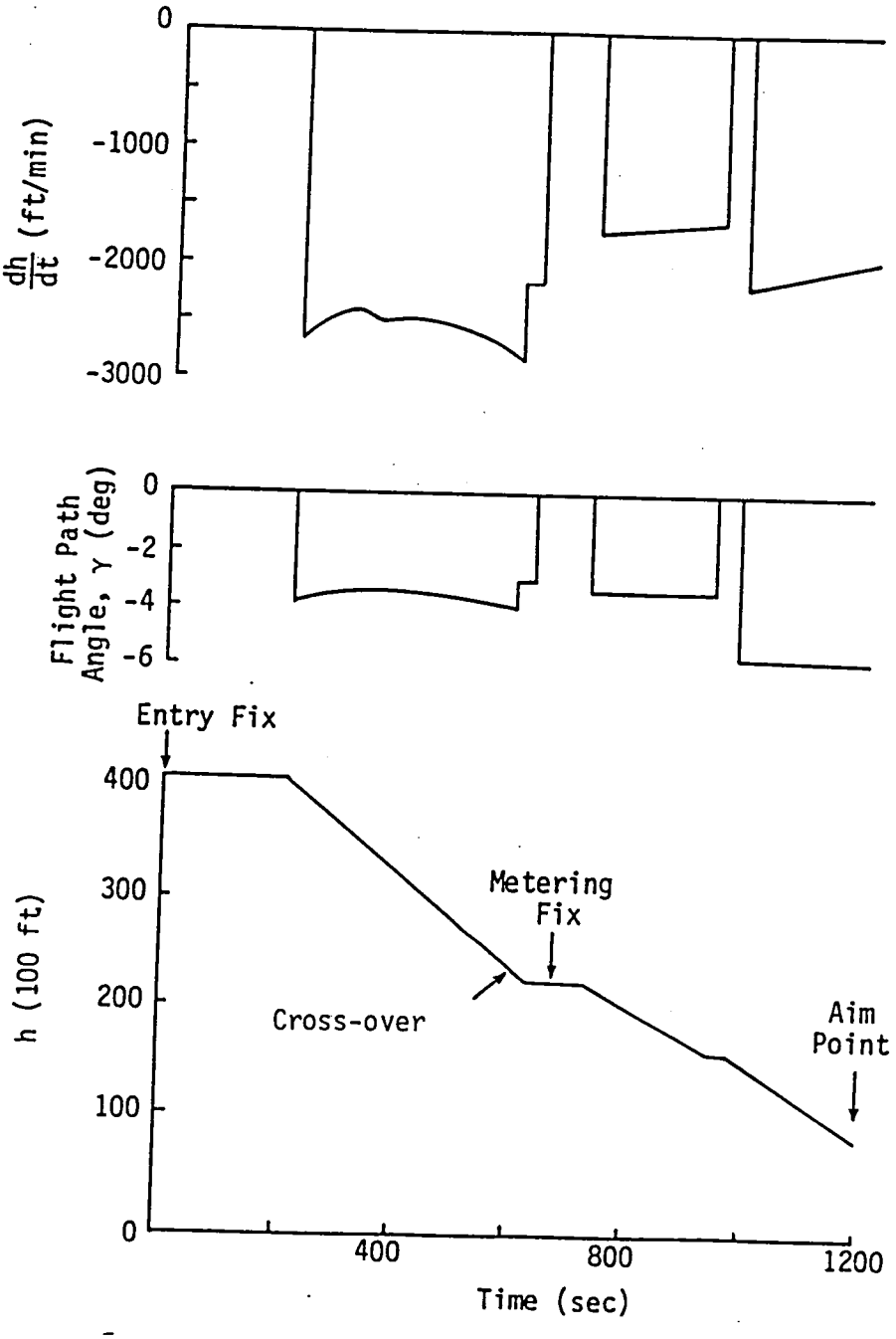

Figure 4-14. Profile descent for B-747 class aircraft.

4.3 Results Using Approximate Relations

To assess the accuracy of the approximate relations given in Eqs. 37 through 46 to calculate Δt_i and ΔS_i, profile descents were calculated and the results are compared below with those from the computer algorithm. The results presented here are for the portion of the flight from the entry fix to the metering fix.

EXAMPLE 1: B-737 - h_c = 35,000 ft, M_c = 0.78, h_{mf} = 19,500 ft, CAS_{ap} = 250 kts, ΔS_{TOT} = 76.049 n.mi., Δt_{req} = 650 sec, θ = 238°, winds in Fig. 4-7, M_d/CAS_d = 0.76/324 kts, T_o = 540° R, p_o = 2116.2 lb/ft^2

Table 4-10. Comparison of calculated and approximate results for B-737.

	Δt_i (sec)		ΔS_i (n.mi.)	
SEGMENT	COMPUTER	APPROX.	COMPUTER	APPROX.
5	8.63	8.38	1.04	1.00
4	303.28	307.51	36.04	36.24
3	155.51	156.45	18.80	18.80
2	112.93	112.65	13.36	13.27
1	68.50	67.41	6.82	6.74
TOTAL	648.85	652.40	76.06	76.05

EXAMPLE 2: B-747 - Same case as listed under Table 4-9.

Table 4-11. Comparison of calculated and approximate results for heavy-class aircraft.

SEGMENT	Δt_i (sec) COMPUTER	Δt_i (sec) APPROX.	ΔS_i (n.mi.) COMPUTER	ΔS_i (n.mi.) APPROX.
5	81.4	79.4	10.01	9.74
4	130.9	134.6	14.39	14.80
3	383.3	381.7	43.02	42.93
2	25.9	25.9	2.98	2.98
1	53.3	52.9	5.64	5.59
TOTAL	674.8	674.5	76.04	76.04

Note that the total distance is the input value in each case because ΔS_4 is calculated such that the total distance is always correct. The results above show that the approximate equations compare well with the computer calculations. However, the rates of descent and decelerations at the end points of each segment were calculated from the same equations as those used in the computer program. Only the region between the end points was approximated. When approximate expressions for the rate of descent, similar to those used in Refs. 2 and 3, were used significant errors would result in some cases. For the B-737 profile descent described in Fig. 15 of Ref. 2, h_c = 35,000 ft. M_c = 0.78, M_d = 0.62, CAS_d = 250 kts = CAS_{mf}, and h_{mf} = 19,500 ft. The rate of descent and time for Segment 3 (M_d=0.62) calculated using the data of Ref. 1 are compared with results using the approximate relations given by Ref. 2:

PARAMETER	CALCULATED FROM DATA IN REF. 1	CALCULATED FROM APPROXIMATE EQUATIONS IN REF. 2
rate of descent (avg)	-2,185 ft/min	-2,638 ft/min
Δt_3	257 sec	213 sec

The time required for Segment 3 is in error by 44 sec out of 257 sec.

Upon reviewing Figure 4 in Ref. 2, it was observed that $M_d = 0.62$ is near the lower end of the curve where the curve-fit could be in error. When the approximate equations of Ref. 2 were applied to the profile descent described above in Example 1, the results compared favorably with the present results. For Segment 3 ($M_d = 0.76$) in that example, a comparison of the two methods is given below:

PARAMETER	CALCULATED FROM DATA IN REF. 1	CALCULATED FROM APPROXIMATE EQUATIONS IN REF. 2
rate of descent at beginning of Segment 3	-3341 ft/min	-3329 ft/min
rate of descent at end of Segment 3	-4320 ft/min	-4523 ft/min
Δt_3	156 sec	150 sec

This favorable comparison is obtained because the curve-fit parameter in Figure 4 of Ref. 2 is close to calculated values for $M_d = 0.76$, whereas the inaccurate value was found for $M_d = 0.62$ in that figure.

5.0 CONCLUSIONS

The following conclusions are drawn from the results obtained in this report:

(1) Uncertainty in descent Mach number had the largest influence on the time required to fly a profile descent, whereas weight had an insignificant influence.

(2) A greater span of control is available when the initial deceleration at cruise altitude occurs before the constant speed segment as opposed to reversing these two segments.

(3) Wind and non-standard atmospheric properties have a large effect on the time involved in a profile descent and therefore should be included in the calculations.

(4) The optimal combination of descent Mach and calibrated airspeed for minimum fuel consumed produces only small savings in fuel. A combination based on flexibility for scheduling seems preferable.

(5) Significant delay capability may be available before the initial descent begins, whereas very little is available while in the descent. Considering the extra work load on the flight crew, it is recommended that profile change commands be given before the descent begins.

(6) Profile descent parameters for heavier aircraft (like the B-747) are similar to those of the B-737.

(7) Errors from using the point-mass trajectory equations and neglecting the transition at the ends of a segment were found to be small. Calculated results compared reasonably well with those from a B-737 flight simulator.

(8) The calculations for time and distance in a segment can be simplified by using approximate relations for the integrals involving the rates of descent and deceleration. However, curve fits to the rates of descent and deceleration were found to be inaccurate in some cases. These rates can be calculated accurately from the point-mass equations.

APPENDIX A
Pressure and Temperature Variation with Altitude

In the stratosphere (below 36,089 ft) the standard temperature is taken to be (Ref. 4):

$$T = T_0 - \alpha h \tag{A-1}$$

where T_0 is sea-level temperature and α is the temperature lapse rate. On a standard day

$$T_0 = 519°R \ (288°K)$$

and

$$\alpha = 3.56616 \times 10^{-3} \ °R/ft$$

The pressure is related to the temperature, and hence altitude, by the relation

$$\frac{p}{p_0} = \left(\frac{T}{T_0}\right)^{5.256114} = \left(\frac{T_0 - \alpha h}{T_0}\right)^{5.256114} \tag{A-2}$$

where p_0 is sea-level pressure.

As noted by Knox and Cannon (Ref. 2), nonstandard temperatures and pressure affect several Mach numbers, airspeed, and altitude relations used in this report. It is assumed that the temperature lapse rate, α, used in Eq. A-1 is not affected by nonstandard days and that only the sea-level temperature, T_0, changes. Eq. A-2 still holds except p_0 must be replaced by p_0^1, the nonstandard sea-level pressure.

For altitudes greater than 36,089 ft, the standard temperature remains constant at T_1 (temperature at 36,089 ft). In this region, the standard pressure is given by Ref. 4 as

$$\frac{p}{p_1} = \exp\left[-g(h-36,089)/RT_1\right] \tag{A-3}$$

where p_1 is the pressure given by Eq. A-2 at 36,089 ft altitude.

APPENDIX B

Mach Number, True, and Calibrated Airspeed Relations

These relations were obtained from Ref. 4. The Mach number is defined by

$$M = \frac{V}{a} \tag{B-1}$$

where a is the local speed of sound,

$$a = \sqrt{\bar{\gamma} R T} \, . \tag{B-2}$$

Here $\bar{\gamma}$ is the ratio of specific heats (1.4 for air), and R is the gas constant for air,

$$R = 1716 \text{ ft}^2/\text{sec}^2 \text{ / } ^\circ\text{R}$$

At subsonic speeds, the ratio of Pitot pressure (p_t) to static pressure (p) is related to the Mach number by

$$\frac{p_t}{p} = \left(1 + \frac{\bar{\gamma}-1}{2} M^2\right)^{\frac{\bar{\gamma}}{\bar{\gamma}-1}} \, . \tag{B-3}$$

This equation can be rearranged to yield

$$M^2 = \frac{2}{(\bar{\gamma}-1)} \left[\left(\frac{p_t - p}{p} + 1 \right)^{\frac{\bar{\gamma}-1}{\bar{\gamma}}} - 1 \right] . \tag{B-4}$$

where $\frac{p_t - p}{p} + 1$ was substituted for $\frac{p_t}{p}$ because airspeed indicators normally measure $(p_t - p)$ instead of p_t alone. Substitute M from Eq. B-1 into Eq. B-4 to obtain the true airspeed squared as

$$V^2 = \frac{2a^2}{\bar{\gamma}-1} \left[\left(\frac{p_t - p}{p} + 1 \right)^{\frac{\bar{\gamma}-1}{\bar{\gamma}}} - 1 \right] . \tag{B-5}$$

Since typical airspeed indicators do not measure a^2 and p individually, they are calibrated using sea-level values for these parameters. With these replacements, the calibrated airspeed squared is obtained from Eq. B-5 as

$$CAS^2 = \frac{2\ a_o^2}{(\bar{\gamma}-1)}\left\{\left[\left(\frac{p_t - p}{p_o}\right)+\ 1\right]^{\frac{\bar{\gamma}-1}{\bar{\gamma}}} -1\right\}. \qquad \text{(B-6)}$$

The calibrated airspeed differs from true airspeed everywhere except at sea level.

True airspeed can be calculated from calibrated airspeed by substituting for $(p_t - p)$ from Eq. B-6 into Eq. B-5 to get

$$V^2 = \frac{2\ a^2}{(\bar{\gamma}-1)}\left\{\left[\ 1\ -\ \frac{p_o}{p} + \frac{p_o}{p}\left(1 + \frac{\bar{\gamma}-1}{2}\ \frac{CAS^2}{a_o^2}\right)^{\frac{\bar{\gamma}}{\bar{\gamma}-1}}\right]^{\frac{\bar{\gamma}-1}{\bar{\gamma}}} -1\right\}. \qquad \text{(B-7)}$$

Divide this equation by a^2 to obtain

$$M^2 = \frac{2}{\bar{\gamma}-1}\left\{\left[1\ -\ \frac{p_o}{p} + \frac{p_o}{p}\left(1 + \frac{\bar{\gamma}-1}{2}\ \frac{CAS^2}{a_o^2}\right)^{\frac{\bar{\gamma}}{\bar{\gamma}-1}}\right]^{\frac{\bar{\gamma}-1}{\bar{\gamma}}} -1\right\}. \qquad \text{(B-8)}$$

Eqs. B-7 and B-8 relate Mach number, true, and calibrated airspeed. The pressure ratio $\frac{p_o}{p}$ is obtained from Eq. A-2 as a function of altitude. Note that p_o and a_o must be standard sea-level values even though the actual sea-level values may be nonstandard.

Cross-Over Altitude

The cross-over altitude is the altitude which gives the cross-over point from the constant Mach descent in Segment 3 to the constant calibrated airspeed-descent in Segment 2. Substitude $\frac{p}{p_o}$ from Eq. A-2 into Eq. B-8 and solve for the cross-over altitude as:

$$h_x = \frac{T_o}{\alpha}\left\{1 - \left[\frac{\left(1 + \frac{\bar{\gamma}-1}{2}\frac{CAS^2}{a_o^2}\right)^{\frac{\bar{\gamma}}{\bar{\gamma}-1}} - 1}{\left(1 + \frac{\bar{\gamma}-1}{2}M^2\right)^{\frac{\bar{\gamma}}{\bar{\gamma}-1}} - 1}\right]^{\frac{1}{5.256114}}\right\} . \qquad \text{(B-9)}$$

For nonstandard days, the term in square brackets above must be multiplied by:

$$\left(\frac{p_o}{p_o^1}\right)^{\frac{1}{5.256114}}$$

to account for nonstandard sea-level pressure in Eq. A-2. Eq. B-9 is restricted to $h_x < 36{,}089$ ft.

If $h_x > 36{,}089$ ft, eq. (A-3) must be used to obtain the cross-over altitude as

$$h_x = 36{,}089 \text{ ft} + \frac{RT_1}{g} \ell n \left(\frac{p_1}{p}\right) \qquad \text{(B-10)}$$

where

$$\frac{p_1}{p} = \frac{p_1}{p_0}\frac{p_0}{p}$$

and Eq. B-8 is used to obtain $\frac{p_o}{p}$ for prescribed values of M and CAS.

APPENDIX C

Relations for dV/dh in Descent Segments

The rate of climb is given by Eq. 7 which requires a relation for dV/dh. This relation is different for constant M and CAS segments. When the calibrated airspeed is maintained constant, differentiate Eq. B-7 with respect to altitude, using Eqs. A-1, A-2, and B-2 to obtain:

$$\frac{dV}{dh} = -\frac{\alpha V}{2T} - \frac{5.256114\ \alpha\ R\ p_o}{V\qquad p}\left[1 - \frac{p_o}{p} + \frac{p_o}{p}\left(1 + \frac{\bar{\gamma}-1}{2}\frac{CAS^2}{a_o^2}\right)^{\frac{\bar{\gamma}}{\bar{\gamma}-1}}\right]^{-\frac{1}{\bar{\gamma}}} \times \left[1 - \left(1 + \frac{\bar{\gamma}-1}{2}\frac{CAS^2}{a_o^2}\right)^{\frac{\bar{\gamma}}{\bar{\gamma}-1}}\right] . \tag{C-1}$$

When the Mach number is maintained constant; differentiate Eq. B-1, using Eqs. B-2 and A-1 to obtain:

$$\frac{dV}{dh} = -\frac{\alpha V}{2T} \tag{C-2}$$

Eqs. C-1 and C-2 are valid for $h < 36{,}089$ ft.

For $h > 36{,}089$ ft, $T = T_1$ = constant and Eq. A-3 must be used in place of Eq. A-2. For constant calibrated airspeed Eq. C-1 must be replaced by

$$\frac{dV}{dh} = \frac{-g}{V}\frac{p_0}{p}\left[1 - \frac{p_0}{p} + \frac{p_0}{p}\left(1 + \frac{\bar{\gamma}-1}{2}\frac{CAS^2}{a_0^2}\right)^{\frac{\bar{\gamma}}{\bar{\gamma}-1}}\right]^{-\frac{1}{\bar{\gamma}}} \times \left[1 - \left(1 + \frac{\bar{\gamma}-1}{2}\frac{CAS^2}{a_0^2}\right)^{\frac{\bar{\gamma}}{\bar{\gamma}-1}}\right] . \quad \text{(C-3)}$$

When the Mach number is constant Eq. C-2 must be replaced by

$$\frac{dV}{dh} = 0 \quad \text{(C-4)}$$

for h > 36,089 ft.

APPENDIX D

Description of Computer Program

The input data required to calculate the profile descent are:

W = weight (lb)

S = wing reference area (ft^2)

TO = sea-level temperature (°R)

PO1 = sea-level pressure (lb/ft^2)

HC = cruise altitude (ft)

HFMAX = maximum metering-fix altitude (ft)

HFMIN = minimum metering-fix altitude (ft)

HAP = aim-point altitude (ft)

DAP = distance from metering fix to aim point (n.mi.)

DSC = distance from metering fix to speed control segment (n.mi.)

VCAP = calibrated airspeed at aim point (kts)

VCSC = calibrated airspeed for speed control (kts)

VCMF = calibrated airspeed at metering fix (kts)

AMC = cruise Mach number

AMMAX = maximum Mach number for aircraft in descent

AMMIN = minimum Mach number for aircraft in descent

VCMX = maximum calibrated airspeed for aircraft in descent (kts)

VCMN = minimum calibrated airspeed for aircraft in descent (kts)

DSTOT = ground distance from entry fix to metering fix (n.mi.)

HDGTRK = track heading from entry fix to metering fix (deg)

TREQ = time required to travel from metering fix to entry fix (sec)

KSEQ = flag; 0 for profile descent as described in this report, 1 for Segments 4 and 5 reversed

WOMEGA = surface wind speed at airport (kts)

WRHO = wind speed gradient at airport (kts/ft)

WPSI = surface wind direction at airport (deg)

WGAM = wind direction gradient at airport (deg/ft)

WSPDB = wind speed bias

WDIRB = wind direction bias

GROUND = altitude of airport above mean sea level (ft)

WGA2 = wind speed at cruise altitude (kts)

WRHO2 = wind speed gradient at cruise altitude (kts/ft)

WPSI2 = wind direction at cruise altitude (deg)

WGAM2 = wind direction gradient at cruise altitude (deg/ft)

HWP = altitude separating two-gradient wind profile (ft)

Drag Data: Drag Coefficient CD as a function of Mach number (AM) and lift coefficient (CL).

Idle-Thrust Data: Engine Thrust (THRUST) as a function of altitude (H) and Mach number (AM).

Fuel Flow Rate: Flow Rate (lb/sec) of fuel as a function of altitude (H), Mach number (AM) and thrust. This information is required only if fuel consumption is desired in the calculation.

The flowchart for the calculations is given on Figure D-1, and the data printed from the computer program are:

1. Input data

2. DAP(MAX) = maximum distance from metering fix to aim point (n.mi.)
   DT(MAX) = maximum time for above (sec)
   DAP(MIN) = minimum distance (n.mi.)
   DT(MIN) = minimum time (sec)

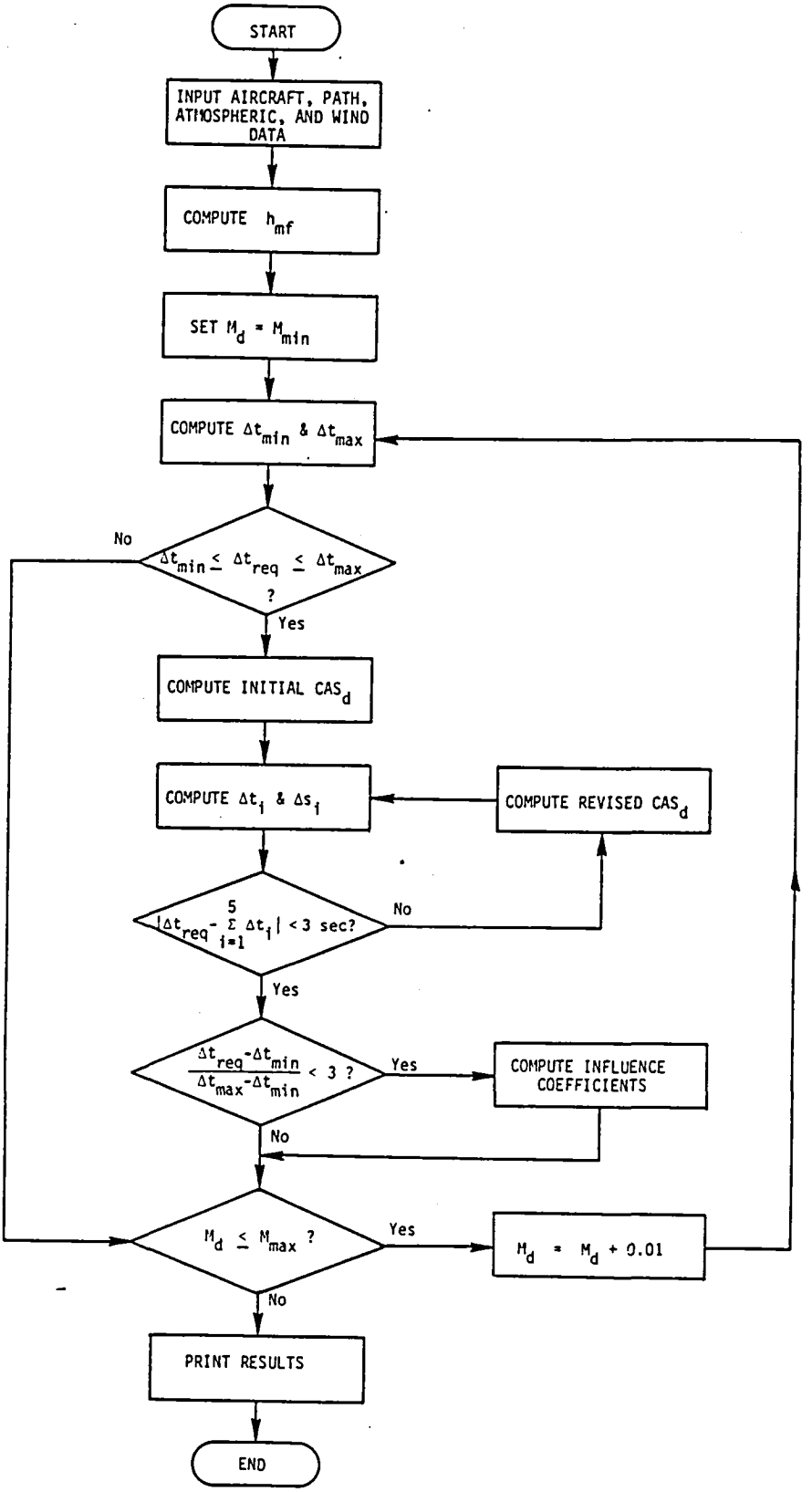

Figure D-1. Flowchart for profile descents.

3. ΔS_i, Δt_i for i = 1A, 2A, 3A, and 4A
   h_{sc} = altitude for speed control (ft)

4. For $M_{min} \leq M_d \leq M_{max}$,
   Δt_{max} Δt_{min} (sec)
   iterations for M_d/CAS_d computation
   CAS_d (kts)
   h_{mf} (ft) h_x (ft)
   ΔS_i (n.mi.), Δt_i (sec), and $\Delta w_{f,i}$ (lbs) for i = 1, ..., 5

5. Influence coefficients

REFERENCES

1. Schwab, R., J. Thompson and J. Grace, "Local Flow Management/Profile Descent Algorithm," Document No. D6-48749, Volumes 1-4, Boeing Commercial Airplane Company, July, 1979.

2. Knox, C. E. and D. G. Cannon, "Development and Test Results of a Flight Management Algorithm for Fuel-Conservative Descents in a Time-Based Metered Traffic Environment," NASA TP-1717, 1980.

3. Knox, C. E., "Planning Fuel-Conservative Descents With or Without Time Constraints Using a Small Programmable Calculator—Algorithm Development and Flight Test Results," NASA TP-2085, February, 1983.

4. Dommasch, D.O., S. S. Sherby and T. F. Connolly, Airplane Aerodynamics, Pitman Publishing Corporation, New York, Fourth Edition, 1967.

5. Conte, S. D. and C. de Boor, Elementary Numerical Analysis, McGraw-Hill, New York, Second Edition, 1972.

6. Britt, C. L., et al, "Study of the Impact of Air Traffic Management Systems on Advanced Aircraft and Avionic Systems," NASA CR-132278, February, 1973.

7. Benoit, A. and S. Swierstra, "Dynamic Control of Inbound Flights for Minimum Cost Operation," AGARD-CP-340, Paper No. 11, October, 1982.

1. Report No.	2. Government Accession No.	3. Recipient's Catalog No.
NASA CR-172338		

4. Title and Subtitle	5. Report Date
Effects of Aircraft and Flight Parameters on Energy-Efficient Profile Descents in Time-Based Metered Traffic	June, 1984
	6. Performing Organization Code
7. Author(s)	8. Performing Organization Report No.
Fred R. DeJarnette	RTI/2467
	10. Work Unit No.
9. Performing Organization Name and Address	
Research Triangle Institute P.O. Box 12194 Research Triangle Park, NC 27709	11. Contract or Grant No. NAS1-17023
	13. Type of Report and Period Covered
12. Sponsoring Agency Name and Address	Contractor Report
National Aeronautics and Space Administration Washington, D.C. 20546	14. Sponsoring Agency Code

15. Supplementary Notes

Langley technical monitor: Leonard Credeur

16. Abstract

The NASA and FAA have developed concepts which save fuel while preserving airport capacity by combining time-based metering with profile descent procedures. A computer algorithm is developed to provide the flight crew with the information needed to fly from an entry fix (about 100 n.mi. from the airport) to a metering fix (about 25 n.mi. from the airport) and arrive there at a predetermined time, altitude, and airspeed. Additional information is calculated for the flight from the metering fix to an aim point near the airport.

The flight path is divided into several descent and deceleration segments. Descents are performed at constant Mach numbers or calibrated airspeed, whereas decelerations occur at constant altitude. The time and distance associated with each segment are calculated from point-mass equations of motion for a clean configuration with idle thrust.

Wind and nonstandard atmospheric properties have a large effect on the flight path. Uncertainty in the descent Mach number was found to have a large effect on the predicted flight time, whereas uncertainty in the weight was insignificant. Of the possible combinations of Mach number and calibrated airspeed for a descent, only small changes were observed in the fuel consumed. Profile descents for the heavier aircraft (like the B-747) were found to be similar to those for the B-737.

17. Key Words (Suggested by Author(s))	18. Distribution Statement
Profile Descent Metered Traffic	Unclassified - Unlimited

19. Security Classif. (of this report)	20. Security Classif. (of this page)	21. No. of Pages	22. Price*
Unclassified	Unclassified	71	

For sale by the National Technical Information Service, Springfield, Virginia 22161